UNCLASSIFIED

AD NUMBER

AD489981

NEW LIMITATION CHANGE

TO

Approved for public release, distribution unlimited

FROM

Distribution authorized to U.S. Gov't. agencies and their contractors; Critical Technology; SEP 1966. Other requests shall be referred to Ballistic Systems and Space Systems Division, Los Angeles, CA.

AUTHORITY

SAMSO ltr, 19 Jan 1972

THIS PAGE IS UNCLASSIFIED

AIR FORCE REPORT NO
SSD-TR-66-73, VOL II

AEROSPACE REPORT NO
TR-669(6220-10)-3, VOL II

Lifting Reentry Communications

Volume II: Systems Calculations

SEPTEMBER 1966

Prepared by
REENTRY AND PLASMA-ELECTROMAGNETICS DEPARTMENT
Plasma Research Laboratory
Laboratories Division
Laboratory Operations
AEROSPACE CORPORATION

Prepared for BALLISTIC SYSTEMS AND SPACE SYSTEMS DIVISIONS
AIR FORCE SYSTEMS COMMAND
LOS ANGELES AIR FORCE STATION
Los Angeles, California

NOTICE

This document is subject to special export controls and each transmittal to foreign governments or foreign nationals may be made only with prior approval of SSD(SSTRT).

Air Force Report No.
SSD-TR-66-73, Vol II

Aerospace Report No.
TR-669(6220-10)-3, Vol II

LIFTING REENTRY COMMUNICATIONS
VOLUME II: SYSTEMS CALCULATIONS

Prepared by
REENTRY AND PLASMA-ELECTROMAGNETICS DEPARTMENT
Plasma Research Laboratory

Laboratories Division
Laboratory Operations
AEROSPACE CORPORATION

September 1966

Prepared for
BALLISTIC SYSTEMS AND SPACE SYSTEMS DIVISIONS
AIR FORCE SYSTEMS COMMAND
LOS ANGELES AIR FORCE STATION
Los Angeles, California

FOREWORD

This report is published by the Aerospace Corporation, El Segundo, California, under Air Force Contract No. AF 04(695)-669. The report was authored by the following members of the ad hoc Working Group on Reentry Communications:

Donald M. Dix
Kurt E. Golden
Edward C. Taylor
Marc A. Kolpin
Paul R. Caron

This working group was organized by Richard H. Huddlestone, Head, Reentry and Plasma-Electromagnetics Department, Plasma Research Laboratory in anticipation of the requirements of the Space Systems Division. The authors gratefully acknowledge Dr. Huddlestone's many suggestions and his constructive criticism.

The following figures have been adapted as indicated: Fig. B-5, from Ref. B-4; Fig. B-6, from Ref. B-5; Fig. B-7, from Ref. B-6; Fig. B-8, from Refs. B-7 and B-8; and Fig. H-1, from Ref. H-1.

This report, which documents research carried out from 1 July 1965 through 1 February 1966, was submitted on 20 September 1966 to Capt. R. F. Jones, SSTRT, for review and approval.

Approved

R. X. Meyer, Director
Plasma Research Laboratory
Laboratories Division
Laboratory Operations

Publication of this report does not constitute Air Force approval of the report's findings or conclusions. It is published only for the exchange and stimulation of ideas.

Robert F. Jones, Captain
Space Systems Division
Air Force Systems Command

ABSTRACT

Calculations supporting the lifting reentry communications systems study are described in this volume. The application and interpretation of these calculations is presented in Volume I of this report. These calculations include the study of lifting reentry trajectories, aerodynamic calculations, signal attenuation, system margins, system modifications, communications fin heat transfer, magnetic window, coolant injection, electrophilic seeding, and quasi-optical and optical systems.

CONTENTS

FIGURES

TABLES

I. INTRODUCTION

This report is the second of three volumes describing the analysis of lifting reentry communications systems. This volume contains the details of investigations that form the basis of the argument in Volume I; Volume III contains an extensive tabulation of transmission and reflection coefficients for a plasma slab.

Each investigation presented in this report has been specifically referred to in Volume I as an appendix, Appendices A through J. These analyses are intended to have meaning only in the context of the total argument presented in Volume I, and this relationship is emphasized in each section of this volume.

APPENDIX A

LIFTING REENTRY TRAJECTORIES

This appendix gives a short derivation of the equations of motion of a gliding reentry vehicle and discusses the assumptions made to obtain the trajectories shown in Figs. 1 through 3 of Volume I, Section II-A-1.

1. EQUATIONS OF MOTION

The flight geometry is illustrated in Fig. A-1. The pertinent symbols are

C_D = drag coefficient

C_L = lift coefficient

D = aerodynamic drag

g = acceleration of gravity, assumed constant

H = altitude above earth surface

L = aerodynamic lift

M = Mach number

m = mass of the R/V

$\overline{R}$ = earth radius

r = radial position of vehicle from center of earth

Re = Reynolds number

S = aerodynamic reference area

T = local temperature

U = magnitude of velocity vector

U_0 = orbital velocity $(r_0 g)^{1/2}$

W = weight of vehicle

α = angle of attack of R/V

θ = path angle

ρ = local density

ρ_s = density at sea level

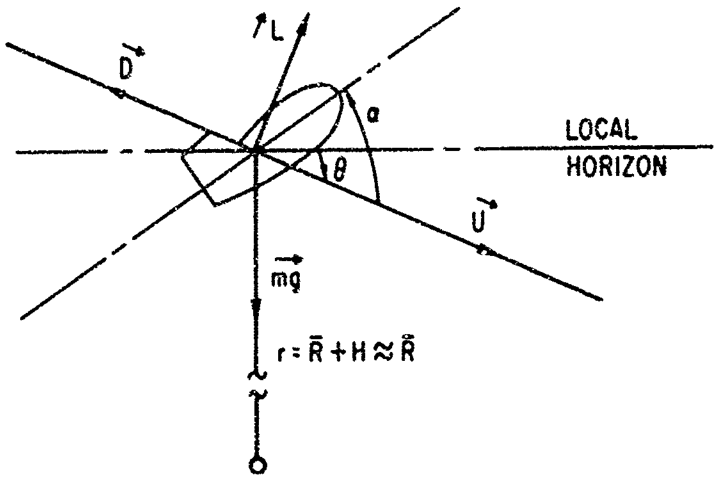

Fig. A-1. Flight Geometry

The definitions

$$L = SC_L \rho U^2/2 \tag{A-1}$$

and

$$D = SC_D \rho U^2/2 \tag{A-2}$$

lead to the equations of motion

$$-\frac{dU}{dt} = -g \sin\theta + \frac{C_D S}{m} \rho \frac{U^2}{2} \tag{A-3}$$

and

$$U \frac{d\theta}{dt} = g \cos \theta - \frac{U^2 \cos \theta}{r} - \frac{C_L S \rho U^2}{2m} \qquad \text{(A-4)}$$

The initial conditions are $t = 0$, $U = U_0$, $\theta = \theta_0$, and $H = H_0$.

The relation $\rho(H)$ may be taken from a standard atmosphere table or be approximated by the isothermal atmosphere

$$\frac{\rho}{\rho_s} = \exp[-(g/RT)H] \qquad \text{(A-5)}$$

The dependence of C_D and C_L on α, Re, and M must be determined for the particular geometry under consideration. The altitude of the R/V as a function of time is given by

$$H = H_0 - \int_0^t U \sin \theta \, dt \qquad \text{(A-6)}$$

2. EQUILIBRIUM TRAJECTORY

An equilibrium lifting reentry trajectory is characterized by a small path angle and a small rate of change in the path angle. Under these circumstances, the equations of motion become

$$\frac{dU}{dt} = \frac{-C_D S}{m} \rho \frac{U^2}{2} \qquad \text{(A-7)}$$

and

$$\frac{U}{U_0} = \left[\frac{r/r_0}{1 + r(C_L S/m)(\rho/2)}\right]^{1/2} \qquad \text{(A-8)}$$

If we introduce $\rho = \rho_s \exp[-(g/RT)H]$, the velocity can be computed as a function of altitude from Eq. (A-8). Integration of Eq. (A-7) will give t(U). For $r = r_0$ = constant, the integration yields

$$t - t_i = \frac{U_0}{2g}\frac{L}{D}\ln\left\{\frac{[1 + (U_i/U_0)]}{[1 - (U_i/U_0)]}\frac{[1 - (U/U_0)]}{[1 + (U/U_0)]}\right\} \qquad \text{(A-9)}$$

Trajectory 1 of Fig. 2, Volume I, has been computed from Eqs. (A-8) and (A 9) using the ARDC Atmosphere Tables.[1] Trajectory 1 corresponds to an entry with U_0 = 25.6 kft/sec, $\theta \approx 0$, and a ballistic parameter W/C_LS of 200 lb/ft^2.

3. NONEQUILIBRIUM TRAJECTORY

As illustrated by Fig. 1, Volume I, a nonzero initial path angle leads to oscillations of the trajectory in the altitude vs velocity plane. To consider the increased depth of blackout encountered during the low-altitude high-velocity pullout, we have defined an idealized and rather extreme nonequilibrium trajectory which is the envelope of trajectories computed by numerically integrating Eqs. (A-3) and (A-4) for $\theta_0 \neq 0$ and W/C_LA = 200 lb/ft^2. The corresponding time scale was determined by observing that the time elapsed from the reentry point is approximately independent of altitude.

[1] The numerical integration of Eqs. (A-7) and (A-8) was originally performed by the General Dynamics Corp., Fort Worth, and the results made available to us by Mr. W. C. Melton of ESTO, Aerospace Corp.

APPENDIX B

AERODYNAMIC CALCULATIONS

This appendix is a compilation of results obtained by the methods described in Volume I, Section II-A-3.

1. OUTER INVISCID FLOW

Figures B-1 through B-4 show the plasma frequency, degree of ionization, and collision frequency in equilibrium air. The plasma frequency and degree of ionization are taken from work by Bleviss (Ref. B-1), which was based on the results of Logan and Treanor (Ref. B-2). The collision frequency was obtained from Bachynski, et al. (Ref. B-3).

Figures B-5 through B-8 show inviscid shock layer properties for cones, wedges, and axisymmetric stagnation points. These figures were adapted as follows: Fig. B-5 from Ref. B-4; Fig. B-6 from Ref. B-5; Fig. B-7 from Ref. B-6; and Fig. B-8 from Refs. B-7 and B-8.

2. VISCOUS BOUNDARY LAYER

The boundary layer properties were obtained from an existing computer program that is described in Ref. B-8. The maximum plasma frequency in the boundary layer on cones and wedges is presented in Figs. B-9 through B-12. Figures B-13 through B-16 show the collision frequency. It is to be noted that these properties differ by as much as 50% from the best available data (see Volume I, II-A-3). The normalized boundary layer thickness $\delta/(x)^{-1/2}$ for wedges is shown in Figs. B-17 through B-20 (The boundary layer thickness in inches is δ, and the distance along the surface of the vehicle measured from the nose in feet is x.); the conical boundary layer thickness is less by a factor of $(3)^{-1/2}$. Figure B-21 presents representative values of the Reynolds number at the boundary layer edge.

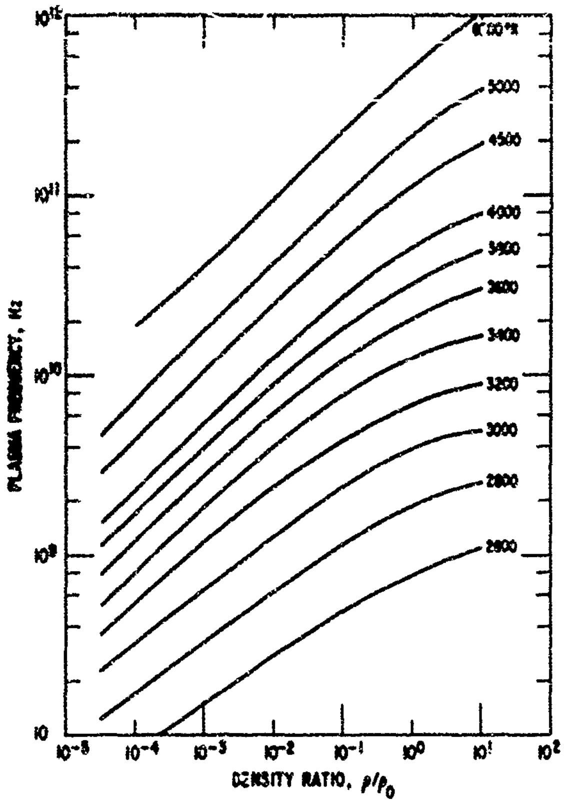

Fig. B-1. Plasma Frequency in Air, Density

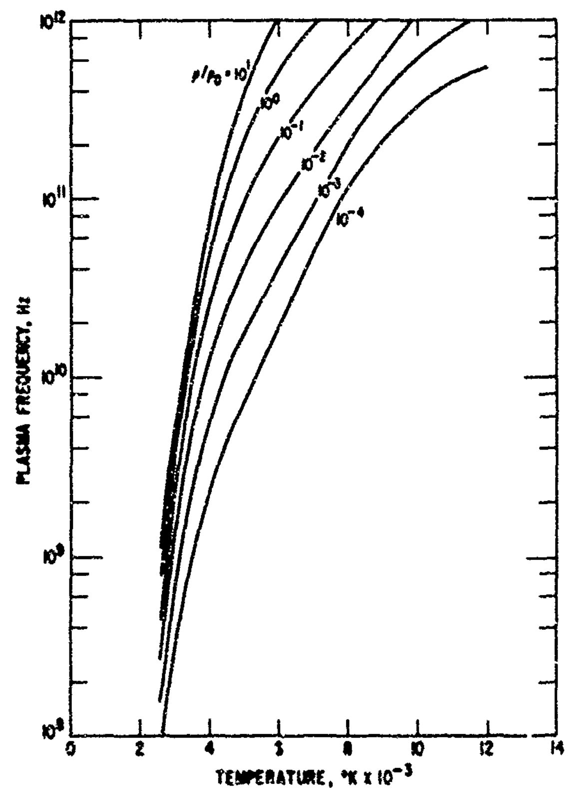

Fig. B-2. Plasma Frequency in Air, Temperature

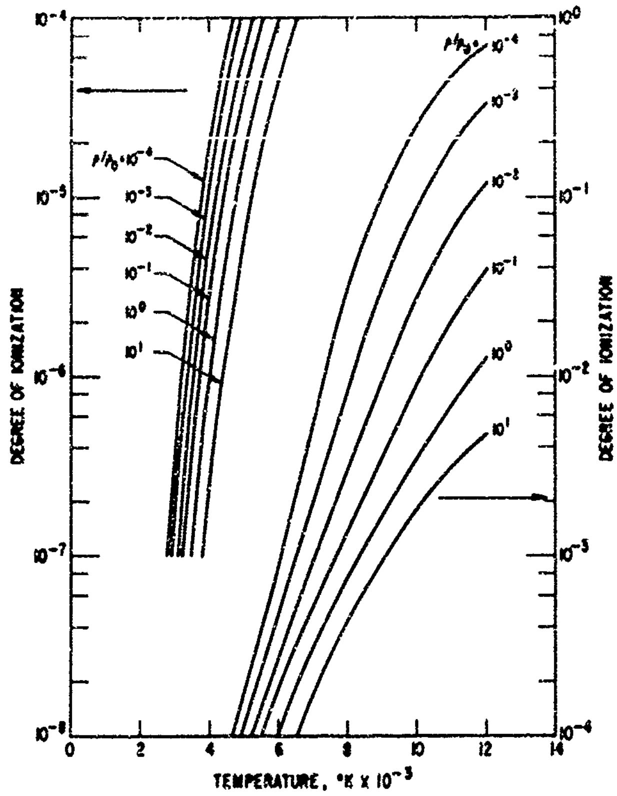

Fig. B-3. Degree of Ionization in Air

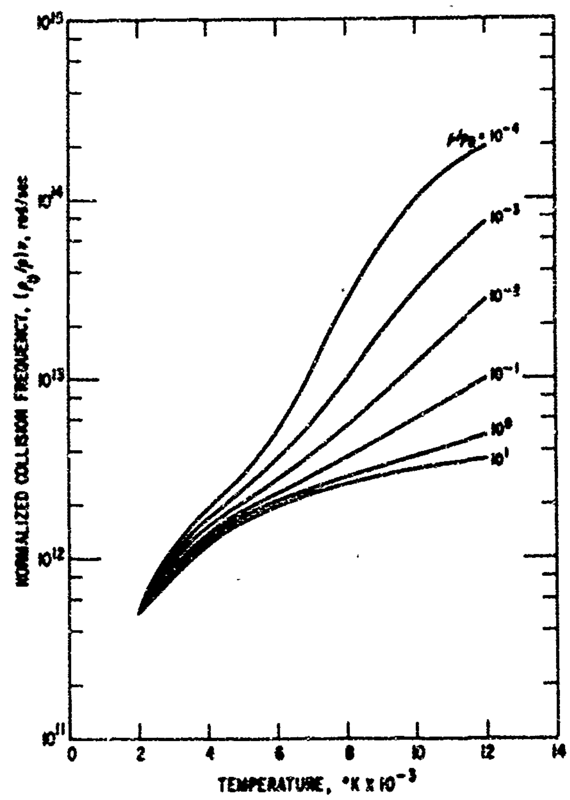

Fig. B-4. Collision Frequency in Air

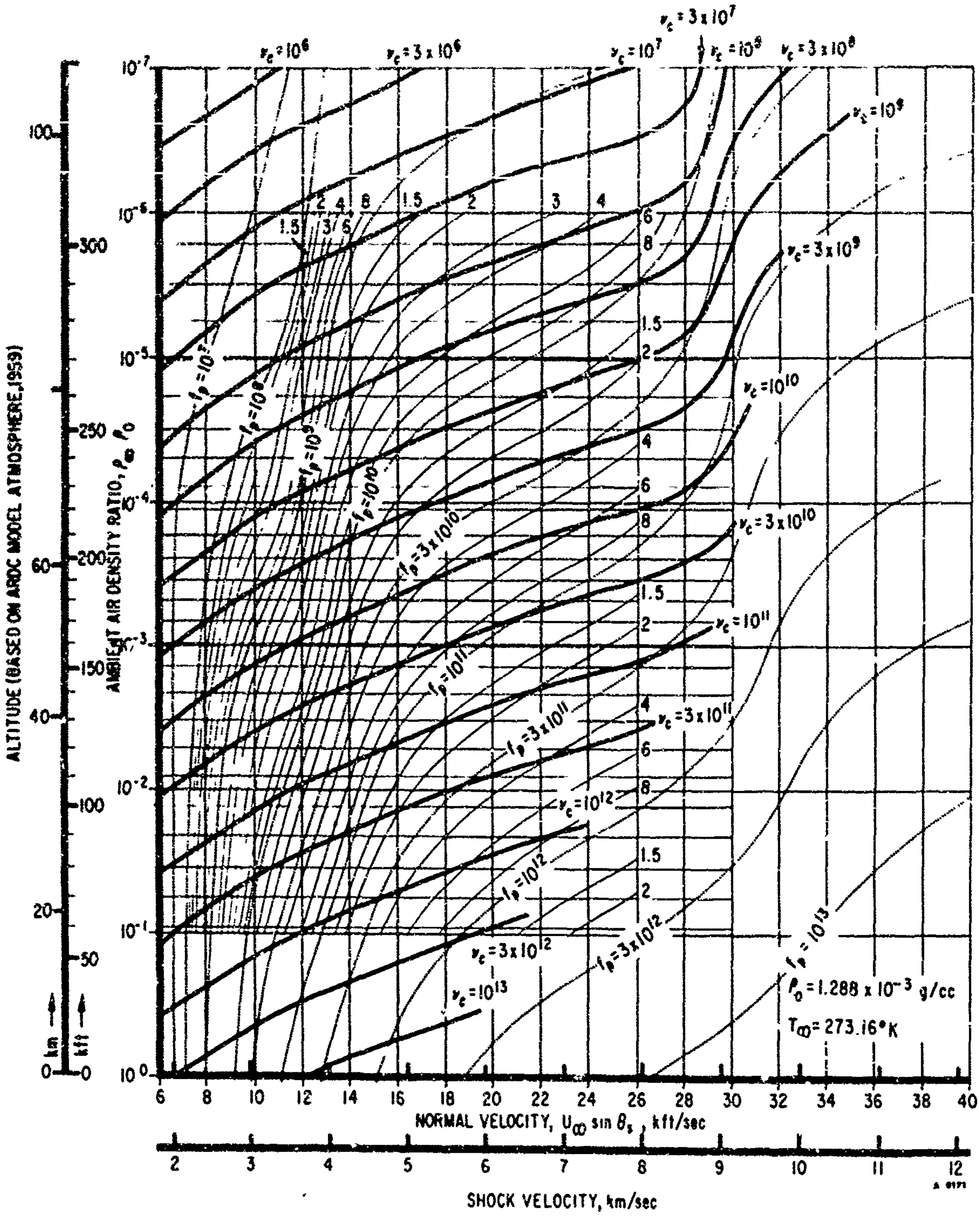

Fig. B-5: Plasma Frequency and Electron Collision Frequency in Equilibrium Air Behind Normal Shocks

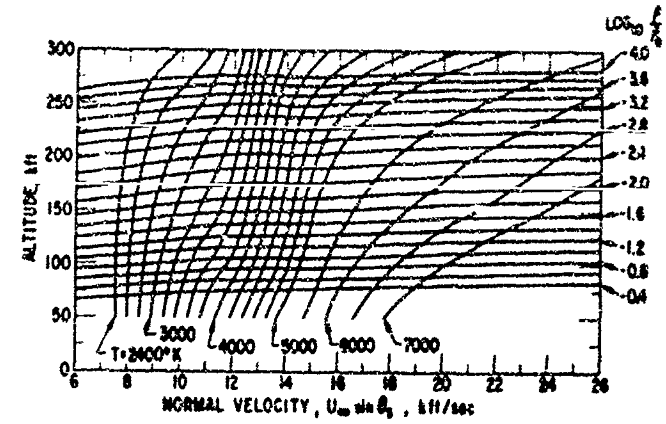

Fig. B-6. Temperature and Density Behind Normal and Oblique Shocks

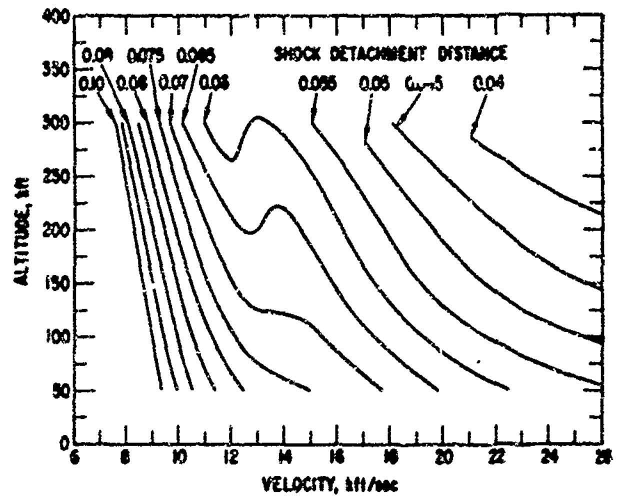

Fig. B-7. Normalized Blunt Body Shock Detachment $\Delta R = 2/\{3[\rho_2/(\rho_1 - 1)]\}$

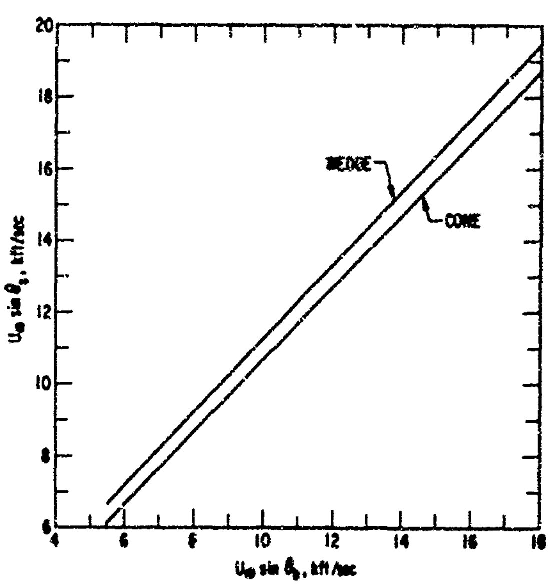

Fig. B-8. Shock Angle vs Body Angle for Wedges and Cones

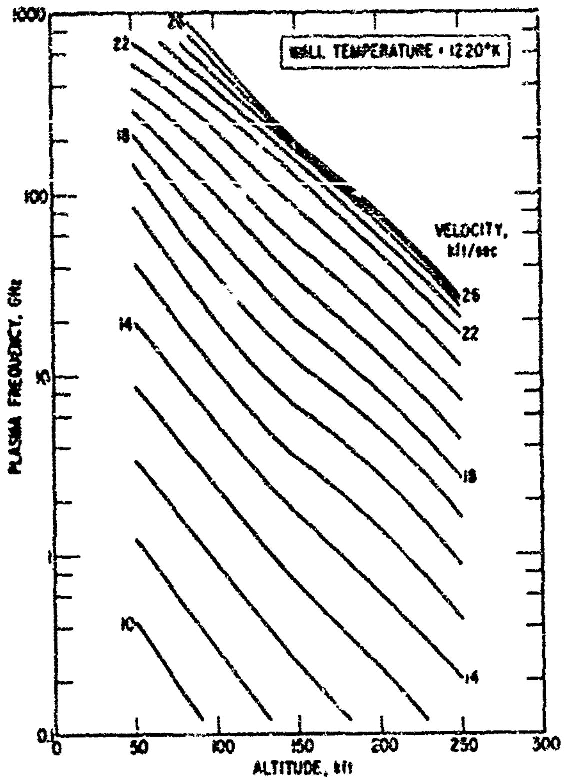

Fig. B-9. Maximum Plasma Frequency in Boundary Layer: Shock Angle = 50 deg

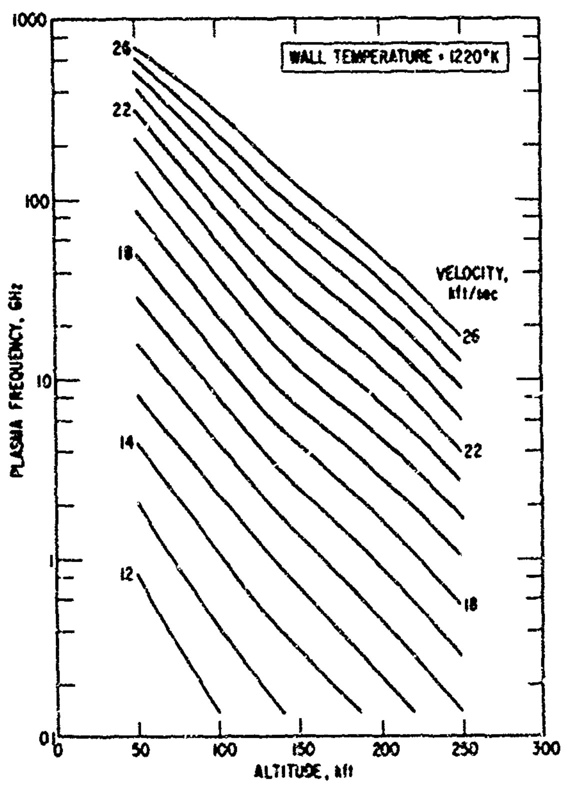

Fig. B-10. Maximum Plasma Frequency in Boundary Layer: Shock Angle = 40 deg

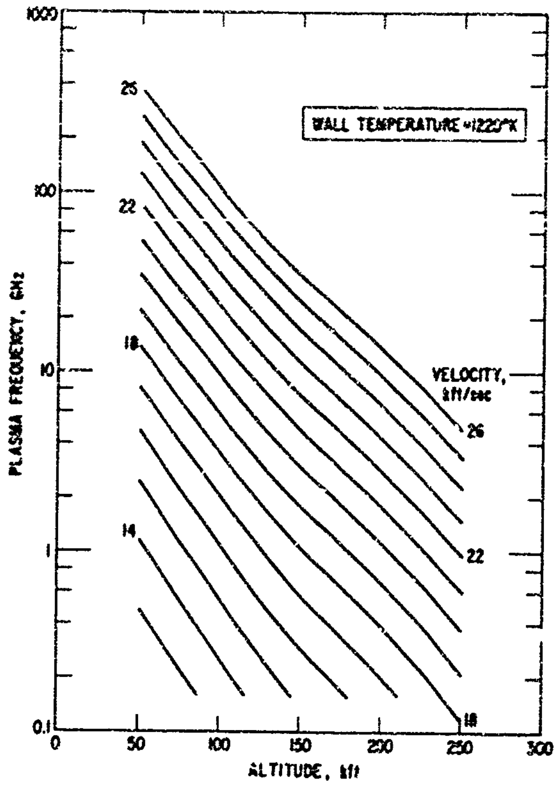

Fig. B-11. Maximum Plasma Frequency in Boundary Layer: Shock Angle = 30 deg

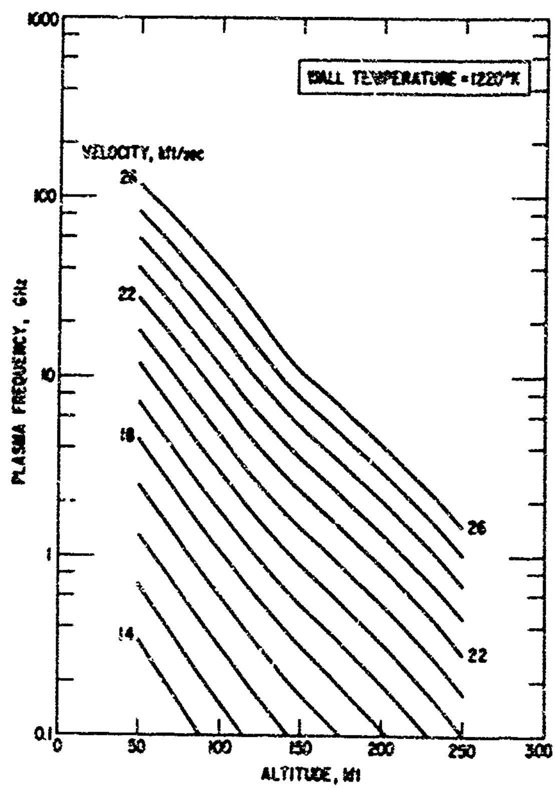

Fig. B-12. Maximum Plasma Frequency in Boundary Layer: Shock Angle = 20 deg

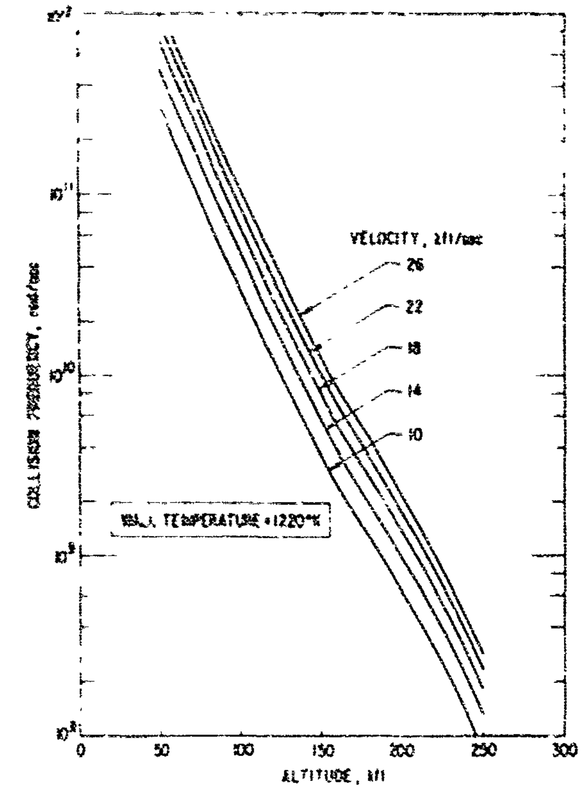

Fig. B-13. Collision Frequency at Peak Boundary Layer Condition: Shock Angle = 50 deg

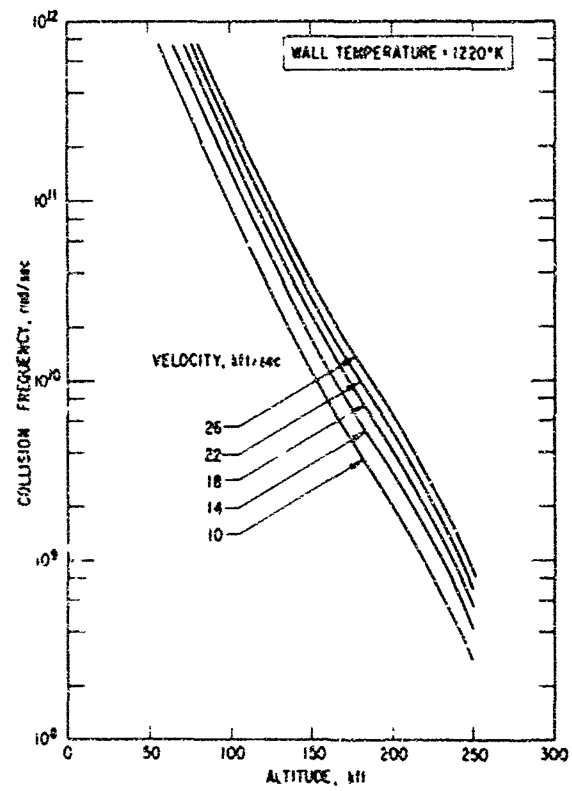

Fig. B-14. Collision Frequency at Peak Boundary Layer Condition: Shock Angle = 40 deg

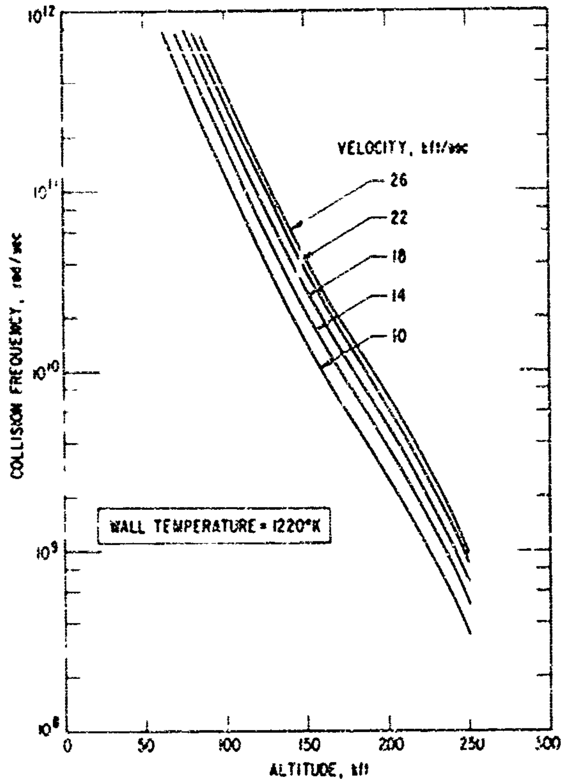

Fig. B-15. Collision Frequency at Peak Boundary Layer Condition: Shock Angle = 30 deg

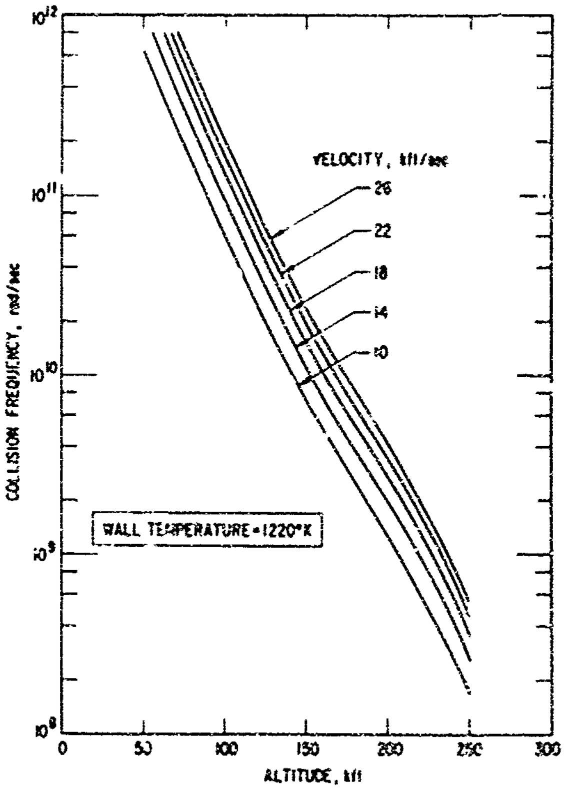

Fig. B-16. Collision Frequency at Peak Boundary Layer Condition: Shock Angle = 20 deg

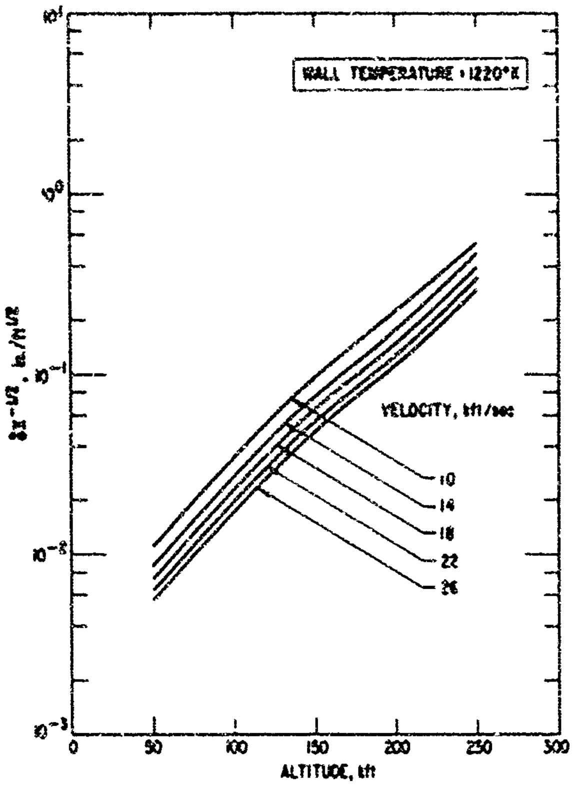

Fig. B-17. Wedge Boundary Layer Thickness (Laminar): Shock Angle = 50 deg

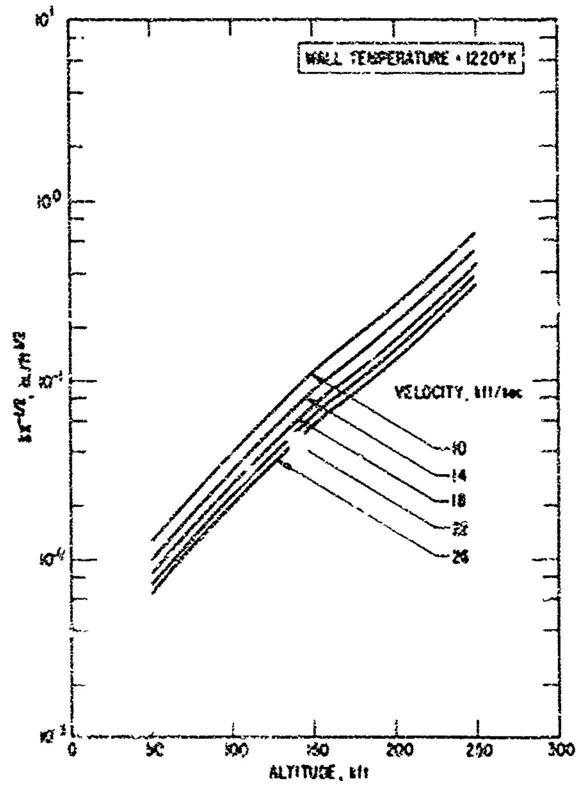

Fig. B-18. Wedge Boundary Layer Thickness (Laminar): Shock Angle = 40 deg

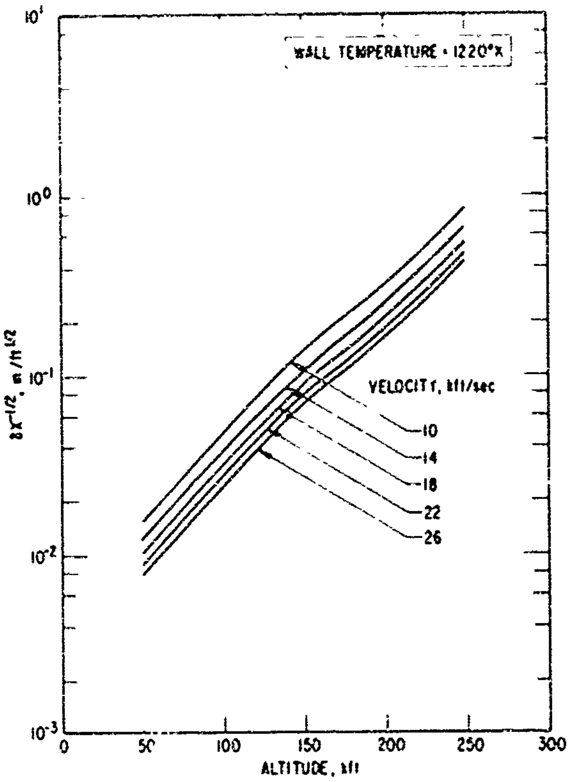

Fig. B-19. Wedge Boundary Layer Thickness (Laminar): Shock Angle = 30 deg

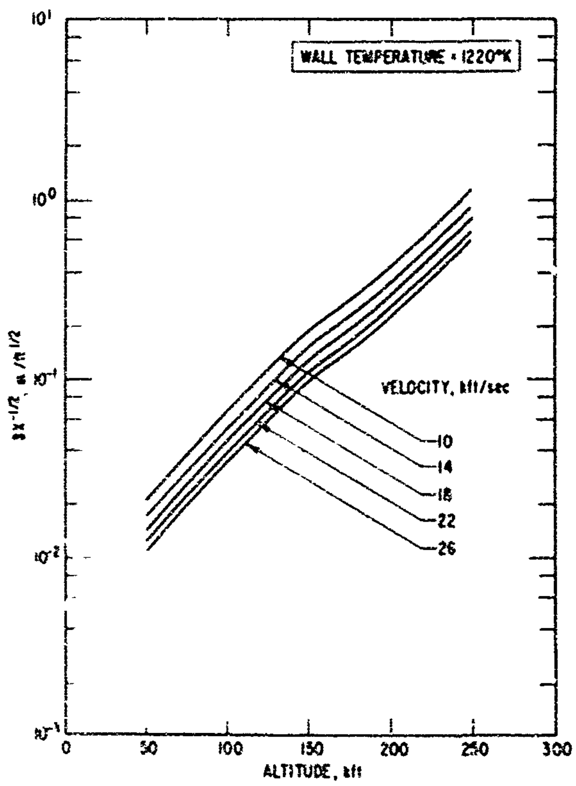

Fig. B-20. Wedge Boundary Layer Thickness (Laminar): Shock Angle = 20 deg

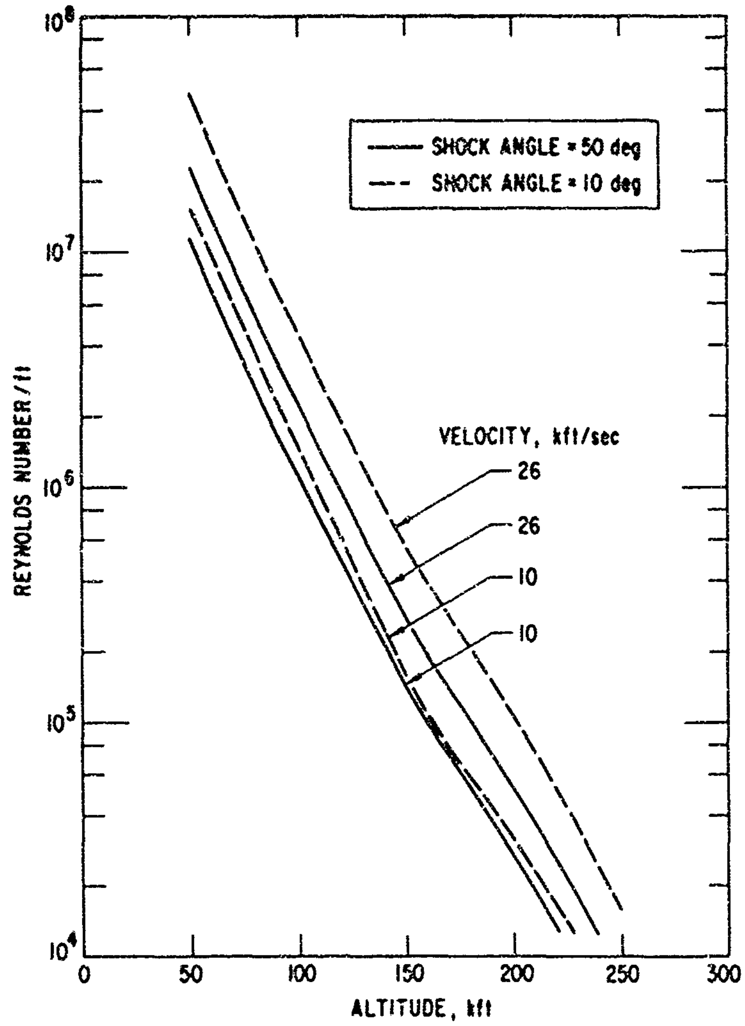

Fig. B-21. Boundary Layer Edge Reynolds Number (per foot) for Wedge

REFERENCES

B-1. Z. O. Bleviss, unpublished work.

B-2. J. G. Logan, Jr., and L. E. Treanor, Tables of Thermodynamic Properties of Air from 3000°K to 10000°K at Intervals of 100°K, BE-1007-3-A, Cornell Aeronautical Lab., Inc., Buffalo, New York (January 1957).

B-3. M. P. Bachynski, T. W. Johnston, and I. W. Shkarofsky, Electromagnetic Properties of High Temperature Air, Proc. IRE 48, 347 (1960).

B-4. H. M. Musal, Jr., Plasma Frequency and Electron Collision Frequency Charts for Hypersonic Vehicle Equilibrium Flow Fields in Air, TR 62-209C, General Motors Corp. Defense Research Lab., Santa Barbara, Calif. (December 1962).

B-5. C. E. Witliff and J. T. Curtis, Normal Shock Wave Parameters in Equilibrium Air, Rept. CAL-111, Cornell Aeronautical Lab., Inc., Buffalo, New York (November 1961).

B-6. H. Serbin, "Supersonic Flow Around Blunt Bodies," J. Aerospace Sci. 25, 58-59 (1958).

B-7. S. Feldman, Hypersonic Gas Dynamic Charts for Equilibrium Air, RR40, Avco-Everett Research Lab., Everett, Mass. (January 1957).

B-8. M. F. Romig, Conical Flow Parameters for Air in Dissociation Equilibrium, RR7, Convair Scientific Research Lab., San Diego, Calif. (May 1960).

APPENDIX C

SIGNAL ATTENUATION

Signal attenuation calculated as indicated in Volume I, Section II-C-1, for cones, wedges, and stagnation points are presented in Tables C-I through C-XIII. The calculations were made for five signal frequencies (0.25, 0.5, 1.0, 5.0, 10 GHz) for representative points along both equilibrium glide and transient trajectories (see Volume I, Section II-A-1). Results are presented according to the following tabulation:

Configuration	Body Station	Flow Field	Table
Stag. Pt.	nose (3-in. radius)	Shock Layer	C-I
Sharp Wedge (50°)	{1 ft, 5 ft}	Shock Layer	C-II
Sharp Wedge (30°, 40°)	{1 ft, 5 ft}	{Shock Layer, Boundary Layer}	C-III, V; C-IV, VI
Sharp Wedge (20°)	{1 ft, 5 ft}	Boundary Layer	C-VII
Sharp Cone (50°)	{1 ft, 5 ft}	Shock Layer	C-VIII
Sharp Cone (30°, 40°)	{1 ft, 5 ft}	{Shock Layer, Boundary Layer}	C-IX, XI; C-X, XII
Sharp Cone (20°)	{1 ft, 5 ft}	Boundary Layer	C-XIII

Table C-XIV presents the characteristic incubation distance for electrons behind plane shock waves in air (Ref. C-1) compared with the appropriate shock layer thicknesses. These data have been used in the discussion of the importance of nonequilibrium effects in Volume I, Section II-C-2.

Table C-I. Stagnation Point Attenuation

Time, sec	Altitude, kft	Velocity kft/sec	f_p, GHz	ω_p rad/sec	d, in.	Attenuation, dB					Traject. 1 = Equil. 2 = Trans.
						f = 250 MHz	f = 500 MHz	f = 1 GHz	f = 5 GHz	f = 10 GHz	
0	308	25.6	6.5	1.5×10^8	0.102	13	6.5	3.8	0.25	0.0	1
100	266	25.0	18.0	1.2×10^9	0.111	29	26.0	22.5	7.8	3.0	1
150	247	24.0	28.0	2.8×10^9	0.118	34	34.0	30.5	18.0	11.0	1
190	236	23.0	32.0	4.0×10^9	0.123	34	35.0	35.0	23.0	15.0	1
230	227	22.0	35.0	5.0×10^9	0.132	35	35.0	36.0	26.0	18.0	1
275	220	21.0	36.0	5.5×10^9	0.136	34	36.0	35.0	28.0	22.0	1
320	214	20.0	37.0	6.2×10^9	0.144	35	36.0	37.0	29.0	23.0	1
365	207	19.0	38.0	7.0×10^9	0.153	35	35.0	38.0	32.0	25.0	1
0	300	25.6	6.5	1.5×10^8	0.102	13	6.5	3.8	0.25	0.0	2
30	280	25.6	13.0	5.5×10^8	0.105	26	20.0	14.0	3.3	1.2	2
60	260	25.6	25.0	1.6×10^9	0.111	36	33.0	28.0	15.0	9.3	2
90	240	25.6	42.0	4.4×10^9	0.117	39	40.0	40.0	28.0	24.0	2
120	220	25.6	65.0	9.8×10^9	0.120	39	41.0	44.0	36.0	39.0	2
150	200	25.6	100.0	2.0×10^{10}	0.123	42	44.0	47.0	62.0	60.0	2
170	200	25.0	95.0	2.0×10^{10}	0.126	41	42.0	46.0	60.0	58.0	2
205	200	24.0	82.0	1.8×10^{10}	0.129	42	40.0	44.0	55.0	53.0	2
240	200	23.0	75.0	1.5×10^{10}	0.132	38	40.0	42.0	54.0	50.0	2
275	200	22.0	65.0	1.5×10^{10}	0.136	36	37.0	40.0	43.0	43.0	2
305	200	21.0	58.0	1.3×10^{10}	0.141	36	38.0	42.0	42.0	40.0	2
340	200	20.0	50.0	1.1×10^{10}	0.147	35	38.0	40.0	40.0	35.0	2
375	200	19.0	43.0	8.2×10^9	0.154	34	38.0	39.0	36.0	28.0	2
410	200	18.0	38.0	8.1×10^9	0.162	35	36.0	38.0	34.0	27.0	1,2
450	194	17.0	37.0	9.1×10^9	0.174	33	35.0	37.0	34.0	28.0	1,2
495	188	16.0	31.0	9.0×10^9	0.183	31	32.0	34.0	30.0	24.0	1,2
540	182	15.0	22.0	8.8×10^9	0.195	26	26.0	27.0	20.0	13.0	1,2
585	176	14.0	16.0	9.0×10^9	0.201	20	20.0	20.0	13.0	7.0	1,2
625	170	13.0	8.0	9.2×10^9	0.201	10	12.0	10.0	2.9	0.7	1,2
670	164	12.0	4.0	9.2×10^9	0.207	4	3.8	3.2	0.3	0.1	1,2

Table C-II. Shock Layer Attenuation, 50-deg Wedge

Time, sec	Altitude, kft	Velocity, kft/sec	f_p, GHz	ν, rad/sec	d(1 ft), in.	d(5 ft), in.	Attenuation, dB f = 250 MHz 1 ft	f = 250 MHz 5 ft	f = 500 MHz 1 ft	f = 500 MHz 5 ft	f = 1 GHz 1 ft	f = 1 GHz 5 ft	f = 5 GHz 1 ft	f = 5 GHz 5 ft	f = 10 GHz 1 ft	f = 10 GHz 5 ft	Traject. 1 = Equil. 2 = Trans
0	300	25.6	3.4	9.0×10^7	1.04	5.22	26.0	91	21.0	85	14.0	71	0.4	0.1	0.0	0.0	1
100	266	25.0	10.0	6.5×10^8	1.09	5.44	63.0	Large	42.0	261	57.0	257	38.0	212.0	10.0	27.0	1
150	247	24.0	17.0	1.5×10^9	1.17	5.85	97.0	Large	96.0	Large	95.0	466	77.0	440.0	63.0	366.0	1
190	236	23.0	20.0	2.2×10^9	1.19	5.95	100.0	Large	104.0	Large	118.0	54	105.0	Large	90.0	472.0	1
230	227	22.0	22.0	2.9×10^9	1.28	6.38	102.0	Large	123.0	Large	130.0	604	128.0	Large	103.0	572.0	1
275	220	21.0	22.0	3.2×10^9	1.34	6.70	100.0	Large	124.0	Large	139.0	643	134.0	Large	110.0	604.0	1
320	214	20.0	21.0	3.8×10^9	1.38	6.90	91.0	Large	117.0	Large	133.0	609	131.0	Large	109.0	561.0	1
365	207	19.0	20.5	4.4×10^9	1.46	7.31	88.0	Large	114.0	Large	133.0	611	139.0	Large	112.0	589.0	1
0	300	25.6	3.4	9.0×10^7	1.04	5.22	26.0	91	21.0	85	7.7	711	0.4	0.5	0.0	< 1	2
30	280	25.6	6.9	3.0×10^8	1.04	5.22	50.0	182	44.0	175	37.0	169	18.0	108.0	0.4	1.0	2
60	260	25.6	13.5	9.8×10^8	1.04	5.22	80.0	Large	79.0	Large	70.0	329	57.0	298.0	38.0	212.0	2
90	240	25.6	22.2	2.5×10^9	1.04	5.42	94.0	Large	106.0	Large	118.0	518	104.0	498.0	80.0	471.0	2
120	220	25.6	35.0	3.6×10^9	1.04	5.22	117.0	Large	148.0	Large	168.0	Large	171.0	Large	159.0	Large	2
150	200	25.6	56.0	1.2×10^{10}	1.04	5.22	100.0	Large	131.0	Large	185.0	Large	260.0	Large	270.0	Large	2
170	200	25.0	55.0	1.2×10^{10}	1.09	5.44	100.0	Large	133.3	Large	181.0	Large	269.0	Large	233.0	Large	2
205	200	24.0	50.0	1.1×10^{10}	1.17	5.85	105.0	Large	138.0	Large	192.0	Large	268.0	Large	265.0	Large	2
240	200	23.0	45.0	9.5×10^9	1.19	5.95	102.0	Large	134.0	Large	184.0	Large	243.0	Large	236.0	Large	2
275	200	22.0	40.0	8.3×10^9	1.28	6.38	103.0	Large	139.0	Large	188.0	Large	230.0	Large	213.0	Large	2
305	200	21.0	34.0	7.3×10^9	1.34	6.70	98.0	Large	125.0	Large	184.0	Large	200.0	Large	206.0	Large	2
340	200	20.0	29.0	6.5×10^9	1.38	6.90	83.0	Large	119.0	Large	160.0	Large	180.0	Large	170.0	Large	2
375	200	19.0	22.0	5.5×10^9	1.46	7.31	80.0	Large	113.0	Large	133.0	612	150.0	Large	128.0	Large	2
410	200	18.0	18.0	4.9×10^9	1.46	7.31	75.0	Large	97.0	Large	123.0	519	115.0	Large	96.0	499.0	1,2
450	194	17.0	14.5	5.5×10^9	1.54	7.72	62.0	236	78.0	Large	93.0	423	94.0	Large	69.0	363.0	1,2
495	188	16.0	9.0	5.5×10^9	1.65	8.25	43.0	159	53.0	223	61.0	281	52.0	275.0	7.9	83.0	1,2
540	182	15.0	5.5	5.8×10^9	1.78	8.88	28.0	101	34.0	138	39.0	180	17.0	82.0	1.6	< 10	1,2
585	176	14.0	3.3	6.1×10^9	1.90	9.50	17.0	61	19.0	83	22.0	105	2.4	12.3	0.5	< 10	1,2
625	170	13.0	2.2	6.5×10^9	2.06	10.30	11.0	43	12.0	57	12.0	68	1.1	< 10	0.2	< 10	1,2
670	164	12.0	1.6	7.2×10^9	2.29	11.40	7.5	30	8.0	38	5.2	31	0.6	< 10	0.0	< 10	1,2

Table C-III. Shock Layer Attenuation, 40-deg Wedge

Time, sec	Altitude, kft	Velocity, kft/sec	f_p, GHz	ν, rad/sec	d(1 ft), in.	d(5 ft), in.	Attenuation, dB: f = 250 MHz, 1 ft	f = 250 MHz, 5 ft	f = 500 MHz, 1 ft	f = 500 MHz, 5 ft	f = 1 GHz, 1 ft	f = 1 GHz, 5 ft	f = 5 GHz, 1 ft	f = 5 GHz, 5 ft	f = 15 GHz, 1 ft	f = 15 GHz, 5 ft	Traject. 1 = Equil. 2 = Trans.
0	300	25.6	2.2	5.9×10^7	0.90	4.50	16.0	52	10.0	49.0	4.0	33.0	0.0	0.0	0.0	0.0	1
100	266	25.0	6.8	4.1×10^8	0.90	4.50	46.0	160	39.0	154.0	35.0	150.0	14.0	88.0	0.1	0.7	1
150	247	24.0	10.5	9.5×10^8	0.94	4.71	61.0	224	58.0	235.0	50.0	222.0	33.0	184.0	13.0	68.0	1
190	236	23.0	12.0	1.4×10^9	0.98	4.92	62.0	231	64.0	263.0	65.0	277.0	46.0	246.0	24.0	135.0	1
230	227	22.0	12.0	1.8×10^9	1.04	5.22	61.0	222	62.3	268.0	69.0	290.0	53.0	270.0	27.0	143.0	1
275	220	21.0	11.0	2.1×10^9	1.04	5.22	57.0	210	55.0	212.0	61.0	265.0	53.0	270.0	19.0	98.0	1
320	214	20.0	9.5	2.4×10^9	1.07	5.34	40.0	134	47.0	175.0	54.5	234.0	35.0	173.0	5.2	12.9	1
365	207	19.0	7.0	3.0×10^9	1.13	5.65	31.0	100	41.0	160.0	40.0	179.0	25.0	119.0	0.5	1.5	1
0	300	25.6	2.2	5.9×10^7	0.90	4.50	16.0	52	10.0	49.0	4.0	33.0	0.0	0.0	0.0	0.0	2
30	280	25.6	4.6	2.0×10^8	0.90	4.50	33.0	111	27.0	107.0	7.0	97.0	2.4	3.1	0.0	0.2	2
60	260	25.6	9.0	6.2×10^8	0.90	4.50	55.0	200	51.0	206.0	46.0	202.0	27.0	150.0	2.0	3.2	2
90	240	25.6	15.0	1.5×10^9	0.90	4.50	73.0	276	77.0	318.0	76.0	333.0	60.0	291.0	42.0	170.0	2
120	220	25.6	24.0	3.5×10^9	0.90	4.50	87.0	305	101.0	Large	108.0	490.0	100.0	400.0	95.0	370.0	2
150	200	25.6	37.0	7.8×10^9	0.90	4.50	80.0	305	150.0	Large	150.0	520.0	165.0	Large	151.0	Large	2
170	200	25.0	34.0	7.0×10^9	0.90	4.50	74.0	300	101.0	Large	145.0	610.2	154.0	690.0	145.0	650.0	2
205	200	24.0	30.0	2.1×10^9	0.94	4.71	130.0	Large	124.0	Large	144.0	650.0	132.0	650.0	121.0	615.0	2
240	200	23.0	26.0	6.0×10^9	0.98	4.92	64.0	234	81.0	329.0	103.0	490.0	107.0	550.0	96.0	520.0	2
275	200	22.0	20.0	5.1×10^9	1.04	5.22	61.0	220	66.5	265.0	95.0	415.0	93.0	440.0	80.0	420.0	2
305	200	21.0	15.5	4.8×10^9	1.04	5.22	49.0	173	59.0	235.0	72.0	317.0	67.0	330.0	52.0	216.0	2
340	200	20.0	12.0	4.1×10^9	1.07	5.34	41.0	136	54.0	226.0	63.0	275.0	53.0	271.0	24.5	110.0	2
375	200	19.0	8.0	3.8×10^9	1.13	5.65	35.0	114	43.0	168.0	45.0	199.0	29.0	160.0	3.4	20.0	2
410	200	18.0	5.00	3.1×10^9	1.17	5.85	19.0	73	28.0	112.0	17.0	125.0	7.0	31.0	0.0	0.5	1,2
450	192	17.0	3.20	3.8×10^9	1.26	6.28	16.0	46	17.0	65.0	13.0	67.0	1.0	4.0	0.0	0.0	1,2
495	188	16.0	1.80	3.9×10^9	1.36	6.80	10.0	35	9.0	42.0	5.0	40.0	0.2	1.0	0.0	0.0	1,2
540	182	15.0	1.30	4.0×10^9	1.44	7.23	5.0	19	5.0	27.0	2.5	22.0	0.1	0.6	0.0	0.0	1,2
585	176	14.3	0.85	4.1×10^9	1.44	7.20	2.0	10	2.4	14.0	1.0	8.5	0.1	0.2	0.0	0.0	1,2
625	170	13.0	0.65	4.5×10^9	1.54	7.72	1.5	7	1.4	8.5	0.6	4.2	0.0	0.2	0.0	0.0	1,2
670	164	12.0	0.40	4.8×10^9	1.67	8.35	1.0	5	0.8	4.0	0.3	2.5	0.0	0.1	0.0	0.0	1,2

Table C-IV. Boundary Layer Attenuation, 40-deg Wedge

Time, sec	Altitude, kft	Velocity, kft/sec	f_p, GHz	ν, rad/sec	d(1 ft), in.	d(5 ft), in.	Attenuation, dB: f = 250 MHz, 1 ft	f = 250 MHz, 5 ft	f = 500 MHz, 1 ft	f = 500 MHz, 5 ft	f = 1 GHz, 1 ft	f = 1 GHz, 5 ft	f = 5 GHz, 1 ft	f = 5 GHz, 5 ft	f = 10 GHz, 1 ft	f = 10 GHz, 5 ft	Traject 1 : Equil 2 : Trans
0	300	25.6	-		-	-	-	-	-	-	-	-	-	-	-	-	1
100	266	25.0	-	-	-	-	-	-	-	-	-	-	-	-	-	-	1
150	247	24.0	16.0	9.8×10^8	0.31	0.70	44.0	71.0	40.0	67.0	34.0	63.0	18.0	45.0	10.0	35.0	1
190	236	23.0	14.5	1.5×10^9	0.26	0.58	35.0	52.0	31.0	53.0	27.0	52.0	13.0	36.0	7.0	23.0	1
230	227	22.0	13.5	2.1×10^9	0.22	0.50	30.0	40.0	29.0	45.0	24.0	36.0	11.0	27.0	5.0	16.0	1
275	220	21.0	10.0	2.6×10^9	0.21	0.46	21.0	29.0	21.0	31.0	18.0	29.0	5.0	15.0	1.4	4.7	1
320	214	20.0	7.4	3.2×10^9	0.19	0.42	16.0	23.0	16.0	23.0	10.0	20.0	1.7	7.3	0.3	1.1	1
365	207	19.0	5.5	3.9×10^9	0.17	0.38	10.0	14.0	8.0	12.0	6.0	11.0	0.5	4.0	0.1	0.3	1
0	300	25.6	-	-	-	-	-	-	-	-	-	-	-	-	-	-	2
30	280	25.6	-	-	-	-	-	-	-	-	-	-	-	-	-	-	2
60	260	25.6	-	-	-	-	-	-	-	-	-	-	-	-	-	-	2
90	240	25.6	26.5	1.6×10^9	0.26	0.59	51.0	83.0	49.0	89.0	44.0	86.0	31.0	72.0	27.0	65.0	2
120	220	25.6	40.0	3.2×10^9	0.18	0.40	48.0	72.0	50.0	80.0	50.0	90.0	38.0	78.0	31.0	74.0	2
150	200	25.6	61.0	6.6×10^9	0.12	0.28	44.0	62.0	45.0	65.0	48.0	81.0	44.0	96.0	36.0	79.0	2
170	200	25.0	52.0	6.5×10^9	0.12	0.28	40.0	55.0	40.0	56.0	42.0	72.0	35.0	70.0	30.0	69.0	2
205	200	24.0	42.0	6.2×10^9	0.13	0.29	37.0	48.0	37.0	50.0	37.0	62.0	25.0	59.0	23.0	55.0	2
240	200	23.0	32.0	6.0×10^9	0.13	0.30	32.0	41.0	31.0	41.0	37.0	48.0	21.0	44.0	15.0	40.0	2
275	200	22.0	23.0	5.8×10^9	0.14	0.30	27.0	35.0	26.0	32.0	23.0	38.0	18.0	36.0	8.0	24.0	2
305	200	21.0	15.0	5.4×10^9	0.14	0.32	21.0	29.0	19.0	24.0	16.0	28.0	8.0	19.0	2.5	11.0	2
340	200	20.0	9.6	5.1×10^9	0.15	0.33	15.0	22.0	13.0	17.0	10.0	20.0	3.0	9.0	0.9	3.0	2
375	200	19.0	6.3	4.9×10^9	0.15	0.33	9.0	15.0	5.0	8.0	5.0	12.6	1.0	3.0	0.2	0.7	2
410	200	18.0	3.90	4.6×10^9	0.15	0.34	4.0	8.0	4.0	8.0	2.2	6.3	0.2	0.5	0.1	0.2	1,2
450	192	17.0	2.90	5.6×10^9	0.14	0.31	3.0	5.0	2.0	4.0	1.2	3.0	0.1	0.3	0.0	0.1	1,2
495	188	16.0	1.80	6.1×10^9	0.13	0.30	1.0	2.0	0.8	1.5	0.4	1.0	0.0	0.1	0.0	0.0	1,2
540	182	15.0	1.10	7.2×10^9	0.13	0.28	0.3	0.6	0.4	0.0	0.2	0.4	0.0	0.0	0.0	0.0	1,2
585	176	14.0	0.56	7.9×10^9	0.12	0.27	0.1	0.2	0.0	0.1	0.0	0.1	0.0	0.0	0.0	0.0	1,2
625	170	13.0	0.28	8.6×10^9	0.11	0.25	0.0	0.0	0.0	0.0	0.0	0.0	0.0	0.0	0.0	0.0	1,2
670	164	12.0	0.12	9.3×10^9	0.11	0.24	0.0	0.0	0.0	2.0	0.0	0.0	3.0	0.0	0.0	0.0	1,2

Table C-V. Shock Layer Attenuation, 30-deg Wedge

Time, sec	Altitude, kft	Velocity, kft/sec	f_p, GHz	ν, rad/sec	d(1 ft), in	d(5 ft), in	Attenuation, dB: f = 250 MHz, 1 ft	f = 250 MHz, 5 ft	f = 500 MHz, 1 ft	f = 500 MHz, 5 ft	f = 1 GHz, 1 ft	f = 1 GHz, 5 ft	f = 5 GHz, 1 ft	f = 5 GHz, 5 ft	f = 10 GHz, 1 ft	f = 10 GHz, 5 ft	Traject 1 = Equil 2 = Trans.
0	300	25.6	0.90	3.0×10^7	0.73	3.66	1.5	13.0	0.45	7.5	0.10	1.8	0.0	0.0	0.0	0.0	1
100	266	25.0	2.00	2.1×10^8	0.73	3.66	10.7	38.5	6.00	32.0	2.70	24.5	0.0	0.0	0.0	0.0	1
150	247	24.0	2.40	5.8×10^8	0.75	3.77	13.5	49.0	8.60	40.0	6.06	39.0	0.1	0.2	0.9	0.0	1
190	235	23.0	2.00	8.0×10^8	0.80	3.98	10.7	40.0	6.40	37.3	3.00	35.5	0.0	0.0	0.0	0.0	1
230	227	22.0	1.50	1.1×10^9	0.84	4.18	5.4	28.0	4.60	24.3	1.70	14.5	0.0	0.0	0.0	0.0	1
275	220	21.0	0.95	1.3×10^9	0.86	4.30	3.8	17.0	1.60	11.0	0.50	4.5	0.0	0.0	0.0	0.0	1
320	214	20.0	0.66	1.4×10^9	0.92	4.60	2.1	10.0	0.83	6.2	0.25	1.5	0.0	0.0	0.0	0.0	1
365	207	19.0	0.60	1.7×10^9	0.96	4.80	1.7	8.4	0.55	3.5	0.20	1.5	0.0	0.0	0.0	0.0	1
0	300	25.6	0.9	3.0×10^7	0.73	3.66	1.3	13.0	0.45	0.75	0.10	1.7	0.0	0.0	0.0	0.0	2
30	280	25.6	1.6	1.0×10^8	0.73	3.66	7.5	37.5	3.40	26.00	1.10	15.5	0.1	0.2	0.0	0.0	2
60	260	25.6	3.0	3.2×10^8	0.73	3.66	19.0	60.0	12.50	52.00	7.80	46.0	0.2	0.4	0.0	0.0	2
90	240	25.6	5.0	9.0×10^8	0.73	3.66	28.0	95.0	23.50	87.00	15.50	85.0	3.0	14.5	0.0	0.3	2
120	220	25.6	7.9	1.9×10^9	0.73	3.66	37.0	113.0	33.50	125.00	32.00	135.0	20.0	98.0	1.0	1.8	2
150	200	25.6	11.0	4.0×10^9	0.73	3.66	39.0	123.0	40.00	147.00	41.00	73.0	29.0	160.0	12.0	75.0	2
170	200	25.0	9.5	3.9×10^9	0.73	3.66	35.5	85.0	36.50	133.00	36.00	150.0	22.7	131.0	6.5	30.0	2
205	200	24.0	6.6	3.5×10^9	0.75	3.77	[illegible]	78.5	24.70	88.50	24.90	105.0	10.0	68.0	0.1	6.0	2
240	200	23.0	4.5	3.1×10^9	0.80	3.98	22.5	71.5	23.00	79.50	22.00	94.0	6.0	40.0	0.0	4.0	2
275	200	22.0	3.0	3.0×10^9	0.84	4.18	13.8	42.0	12.00	47.00	9.50	48.0	0.2	0.3	0.0	1.0	2
305	200	21.0	1.7	2.5×10^9	0.86	4.30	8.0	22.5	5.50	24.00	2.90	21.5	0.1	0.1	0.0	0.0	2
340	200	20.0	1.0	2.3×10^9	0.92	4.60	3.0	12.0	2.20	13.00	0.85	7.0	0.0	0.0	0.0	0.0	2
375	200	19.0	0.7	2.2×10^9	0.96	4.80	1.5	7.0	1.10	6.80	0.40	2.6	0.0	0.0	0.0	0.0	2
410	200	18.0	0.50	2.0×10^9	0.96	4.80	1.10	5.60	0.5	3.2	0.2	0.90	0.0	0.0	0.0	0.0	1,2
450	192	17.0	0.40	2.2×10^9	0.98	4.92	0.45	2.40	0.3	1.9	0.1	0.50	0.0	0.0	0.0	0.0	1,2
495	18[illegible]	16.0	0.31	2.3×10^9	1.07	5.34	0.35	2.00	0.2	1.2	0.1	0.35	0.0	0.0	0.0	0.0	1,2
540	182	15.0	0.20	2.2×10^9	1.15	5.75	0.10	1.00	0.1	0.5	0.0	0.20	0.0	0.0	0.0	0.0	1,2
585	176	14.0	0.13	2.5×10^9	1.21	6.05	0.10	0.39	0.0	0.2	0.0	0.10	0.0	0.0	0.0	0.0	1,2
625	170	13.0	0.08	2.5×10^9	1.32	6.58	0.00	0.25	0.0	0.1	0.0	0.00	0.0	0.0	0.0	0.0	1,2
670	164	12.0	-	-	-	-	-	-	-	-	-	-	-	-	-	-	1,2

Table C-VI. Boundary Layer Attenuation, 30-deg Wedge

Time, sec	Altitude, kft	Velocity, kft/sec	f_p, GHz	ν, rad/sec	d(1 ft), in.	d(5 ft), in.	Attenuation, dB: f = 250 MHz, 1 ft	f = 250 MHz, 5 ft	f = 500 MHz, 1 ft	f = 500 MHz, 5 ft	f = 1 GHz, 1 ft	f = 1 GHz, 5 ft	f = 5 GHz, 1 ft	f = 5 GHz, 5 ft	f = 10 GHz, 1 ft	f = 10 GHz, 5 ft	Traject 1 = Equil 2 = Trans
0	300	25.6	-	-	-	-	-	-	-	-	-	-	-	-	-	-	1
100	266	25.3	-	-	-	-	-	-	-	-	-	-	-	-	-	-	1
150	247	24.0	4.00	6.9×10^8	0.20	0.45	11.0	19.0	6.7	13.9	2.7	8.4	0.2	0.6	0.0	0.0	1
190	236	23.0	3.45	1.1×10^9	0.31	0.70	11.6	19.0	8.3	15.5	4.4	10.0	0.2	0.5	0.0	0.0	1
230	227	22.0	2.85	1.5×10^9	0.27	0.59	7.8	14.6	4.3	10.0	1.8	6.2	0.1	0.2	0.0	0.0	1
275	220	21.0	2.10	1.9×10^9	0.24	0.54	5.9	7.9	2.4	4.8	1.0	2.0	0.0	0.1	0.0	0.0	1
320	214	20.0	1.55	2.3×10^9	0.22	0.49	2.0	4.7	1.3	2.6	0.5	1.2	0.0	0.0	0.0	0.0	1
365	207	19.0	1.11	2.9×10^9	0.20	0.44	1.1	2.4	0.7	1.7	0.3	0.6	0.0	0.0	0.0	0.0	1
0	300	25.6	-	-	-	-	-	-	-	-	-	-	-	-	-	-	2
30	280	25.6	-	-	-	-	-	-	-	-	-	-	-	-	-	-	2
60	260	25.6	-	-	-	-	-	-	-	-	-	-	-	-	-	-	2
90	240	25.6	9.50	1.0×10^9	0.32	0.71	31.0	47.0	27.0	43.0	22.00	38.0	7.2	21.5	2.00	4.7	2
120	220	25.6	12.50	2.4×10^9	0.21	0.48	26.0	38.0	25.0	33.0	21.00	36.0	8.4	21.9	3.70	11.0	2
150	200	25.6	19.50	5.0×10^9	0.14	0.32	25.0	35.0	25.0	33.0	21.00	37.0	13.0	28.0	5.80	23.0	2
170	200	25.0	16.00	4.8×10^9	0.15	0.33	22.0	32.0	22.0	32.0	18.00	33.0	8.9	21.0	4.00	13.3	2
205	200	24.0	10.80	4.6×10^9	0.15	0.34	16.0	23.5	16.0	23.0	12.00	23.0	4.6	10.0	1.40	5.1	2
240	200	23.0	7.30	4.4×10^9	0.16	0.35	13.0	17.0	11.5	17.0	5.50	15.0	1.2	4.3	0.45	0.8	2
275	190	22.0	4.95	4.1×10^9	0.16	0.35	9.0	13.0	7.5	12.5	3.40	9.0	0.4	1.3	0.10	0.3	2
305	200	21.9	3.15	4.0×10^9	0.17	0.37	5.3	8.7	3.0	6.7	1.20	3.8	0.1	0.3	0.00	0.1	2
340	200	20.0	2.10	3.8×10^9	0.17	0.38	2.4	4.3	1.5	3.4	0.50	1.6	0.0	0.1	0.00	0.0	2
375	200	19.0	1.28	3.6×10^9	0.18	0.39	1.0	2.0	0.7	1.5	0.30	0.5	0.0	0.0	0.00	0.0	2
410	200	18.0	0.74	3.4×10^9	0.38	0.40	0.4	0.8	0.2	0.6	0.0	0.1	0.0	0.0	0.0	0.0	1,2
450	192	17.0	0.47	4.1×10^9	0.16	0.36	0.1	0.2	0.1	0.2	0.0	0.0	0.0	0.0	0.0	0.0	1,2
495	188	16.4	0.28	4.5×10^9	0.16	0.36	0.0	0.1	0.0	0.0	0.0	0.0	0.0	0.0	0.0	0.0	1,2
540	182	15.9	0.16	5.2×10^9	0.15	0.33	0.0	0.0	0.0	0.0	0.0	0.0	0.0	0.0	0.0	0.0	1,2
585	176	14.0	-	-	-	-	-	-	-	-	-	-	-	-	-	-	1,2
625	170	13.0	-	-	-	-	-	-	-	-	-	-	-	-	-	-	1,2
670	164	12.0	-	-	-	-	-	-	-	-	-	-	-	-	-	-	1,2

Table C-VII. Boundary Layer Attenuation, 20-deg Wedge

Time, sec	Altitude, kft	Velocity, kft/sec	f_p, GHz	ν, rad/sec	d(1 ft), in.	d(5 ft), in.	Attenuation, dB: f = 250 MHz, 1 ft	f = 250 MHz, 5 ft	f = 500 MHz, 1 ft	f = 500 MHz, 5 ft	f = 1 GHz, 1 ft	f = 1 GHz, 5 ft	f = 5 GHz, 1 ft	f = 5 GHz, 5 ft	f = 10 GHz, 1 ft	f = 10 GHz, 5 ft	Traject 1 = Equil 2 = Trans.
0	300	25.6	-	-	-	-	-	-	-	-	-	-	-	-	-	-	1
100	266	25.0	-	-	-	-	-	-	-	-	-	-	-	-	-	-	1
150	247	24.0	1.010	3.7×10^8	0.50	1.10	1.7	4.0	0.5	1.4	0.2	0.6	-	-	-	-	1
190	236	23.0	0.860	6.2×10^8	0.40	0.91	1.2	3.3	0.4	1.1	0.1	0.3	-	-	-	-	1
230	227	22.0	0.710	8.5×10^8	0.36	0.80	0.7	2.0	0.3	0.5	0.0	0.1	-	-	-	-	1
275	220	21.0	0.520	1.1×10^9	0.32	0.72	0.3	1.1	0.1	0.3	0.0	0.1	-	-	-	-	1
320	214	20.0	0.375	1.3×10^9	0.30	0.66	0.2	0.4	0.1	0.2	0.0	0.1	-	-	-	-	1
365	207	19.0	0.265	1.5×10^9	0.26	0.59	0.1	0.2	0.0	0.1	0.0	0.0	-	-	-	-	1
0	300	25.6	-	-	-	-	-	-	-	-	-	-	-	-	-	-	2
30	280	25.6	-	-	-	-	-	-	-	-	-	-	-	-	-	-	2
60	260	25.6	-	-	-	-	-	-	-	-	-	-	-	-	-	-	2
90	240	25.6	2.350	5.4×10^8	0.43	0.96	10.2	17.0	5.6	11.0	1.7	5.6	0.0	0.0	-	-	2
120	220	25.6	3.250	1.2×10^9	0.29	0.64	10.1	16.0	6.0	12.0	3.3	7.8	0.1	0.3	-	-	2
150	200	25.6	4.800	2.6×10^9	0.19	0.43	11.0	16.0	8.1	15.0	4.1	10.4	0.2	1.0	-	-	2
170	200	25.0	3.950	2.5×10^9	0.20	0.45	8.5	12.0	6.2	12.0	3.8	8.3	0.1	0.6	-	-	2
205	200	24.0	2.790	2.4×10^9	0.20	0.46	5.1	9.6	3.2	7.3	1.6	4.4	0.0	0.1	-	-	2
240	200	23.0	1.850	2.4×10^9	0.21	0.47	2.5	5.6	1.5	3.1	0.8	1.9	0.0	0.0	-	-	2
275	200	22.0	1.250	2.2×10^9	0.21	0.48	1.2	2.8	0.7	1.7	0.3	0.7	0.0	0.0	-	-	2
305	200	21.0	0.800	2.2×10^9	0.22	0.50	0.8	1.9	0.5	1.1	0.2	0.4	0.0	0.0	-	-	2
340	200	20.0	0.505	2.1×10^9	0.23	0.51	0.2	0.4	0.1	0.3	0.0	0.1	0.0	0.0	-	-	2
375	200	19.0	0.310	2.0×10^9	0.24	0.53	0.1	0.2	0.0	0.1	0.0	0.0	0.0	0.0	-	-	2
410	200	18.0	0.182	1.9×10^9	0.24	0.54	0.0	0.1	0.0	0.0	0.0	0.0					1,2
450	194	17.0	-	-	-	-	-	-	-	-	-	-	-	-	-	-	1,2
495	188	16.0	-	-	-	-	-	-	-	-	-	-	-	-	-	-	1,2
540	182	15.0	-	-	-	-	-	-	-	-	-	-	-	-	-	-	1,2
585	176	14.0	-	-	-	-	-	-	-	-	-	-	-	-	-	-	1,2
625	170	13.0	-	-	-	-	-	-	-	-	-	-	-	-	-	-	1,2
670	164	12.0	-	-	-	-	-	-	-	-	-	-	-	-	-	-	1,2

Table C-VIII. Shock Layer Attenuation, 50-deg Cone

Time, sec	Altitude, kft	Velocity, kft/sec	f_p, GHz	ν, rad/sec	d(1 ft), in.	d(5 ft), in.	Attenuation, dB: f = 250 MHz, 1 ft	f = 250 MHz, 5 ft	f = 500 MHz, 1 ft	f = 500 MHz, 5 ft	f = 1 GHz, 1 ft	f = 1 GHz, 5 ft	f = 5 GHz, 1 ft	f = 5 GHz, 5 ft	f = 10 GHz, 1 ft	f = 10 GHz, 5 ft	Traject. 1 = Equil. 2 = Trans.
0	300	25.6	2.9	7.5×10^{7}	0.52	2.62	14.0	44.0	8.6	38.0	4.2	29.0	0.2	0.1	0.0	0.1	1
100	26[illegible]	25.0	9.2	6.0×10^{8}	0.54	2.72	41.0	130.0	35.0	137.0	30.0	122.0	14.0	92.0	3.0	5.9	1
150	247	24.0	15.5	1.4×10^{9}	0.58	2.92	57.0	186.0	57.0	210.0	53.0	219.0	38.0	198.0	26.0	155.0	1
190	236	23.0	18.0	2.0×10^{9}	0.58	2.92	59.0	211.0	62.0	235.0	60.0	249.0	47.0	234.0	36.0	199.0	1
230	227	22.0	19.5	2.6×10^{9}	0.58	2.92	57.0	190.0	63.0	239.0	64.0	263.0	51.0	256.0	43.0	223.0	1
275	220	21.0	18.0	2.7×10^{9}	0.65	3.25	57.0	199.0	63.0	239.0	64.0	267.0	52.0	257.0	40.0	220.0	1
320	214	20.0	18.0	3.3×10^{9}	0.71	3.56	55.0	188.0	63.0	247.0	67.0	283.0	56.0	272.0	44.0	240.0	1
365	207	19.0	17.0	4.0×10^{9}	0.73	3.66	49.0	167.0	58.0	225.0	62.0	249.0	54.0	273.0	41.0	227.0	1
0	300	25.6	2.9	7.5×10^{7}	0.52	2.62	14.0	44.0	8.8	38.0	4.2	29.0	0.2	0.1	0.0	0.1	2
30	280	25.6	6.2	2.7×10^{8}	0.52	2.62	30.0	91.0	24.0	84.0	18.0	77.0	4.3	39.0	0.3	0.4	2
60	260	25.6	12.0	9.0×10^{8}	0.52	2.62	47.0	152.0	47.0	155.0	38.0	152.0	23.0	[illegible]	11.0	74.0	2
90	240	25.6	20.5	2.2×10^{9}	0.52	2.62	58.0	198.0	62.0	232.0	61.0	247.0	48.0	[illegible]	38.0	210.0	2
120	220	25.6	33.0	5.0×10^{9}	0.52	2.62	61.0	203.0	74.0	296.0	83.0	348.0	81.0	[illegible]	74.0	374.0	2
150	200	25.6	52.0	1.1×10^{10}	0.52	2.62	62.0	207.0	76.0	288.0	98.0	405.0	129.0	[illegible]	126.0	Large	2
170	200	25.0	50.0	1.05×10^{10}	0.54	2.72	62.0	210.0	77.0	288.0	97.0	419.0	128.0	603.0	124.0	Large	2
205	200	24.0	44.0	9.5×10^{9}	0.58	2.92	62.0	210.0	77.0	295.0	98.0	422.0	122.0	583.0	117.0	580.0	2
240	200	23.0	40.0	8.2×10^{9}	0.58	2.92	62.0	210.0	77.0	294.0	96.0	407.0	111.0	534.0	106.0	525.0	2
275	200	22.0	34.0	7.2×10^{9}	0.58	2.92	58.0	172.0	70.0	265.0	86.0	365.0	95.0	484.0	87.0	440.0	2
305	200	21.0	30.0	6.5×10^{9}	0.65	3.25	58.0	196.0	70.0	280.0	66.0	362.0	91.0	443.0	83.0	421.0	2
340	200	20.0	25.0	3.7×10^{9}	0.71	3.56	56.0	192.0	69.0	268.0	79.0	337.0	82.0	397.0	72.0	371.0	2
375	200	19.0	18.0	5.0×10^{9}	0.73	3.66	47.0	157.0	56.0	215.0	63.0	266.0	58.0	288.0	46.0	247.0	2
410	200	18.0	14.0	4.2×10^{9}	0.75	3.76	42.0	139.0	50.0	188.0	53.0	223.0	43.0	223.0	28.0	165.0	1, 2
450	194	17.0	9.5	5.0×10^{9}	0.80	3.98	31.0	92.0	35.0	135.0	36.0	159.0	25.0	142.0	6.6	30.0	1, 2
495	188	16.0	6.0	5.0×10^{9}	0.86	4.29	22.0	64.0	23.3	86.0	23.0	101.0	9.5	62.0	0.6	4.5	1, 2
540	182	15.0	3.4	6.0×10^{9}	1.00	5.00	14.0	41.0	14.0	54.0	12.0	62.0	1.5	7.1	0.3	<1.0	1, 2
585	176	14.0	2.0	5.5×10^{9}	1.00	5.00	6.7	22.0	6.7	27.0	4.9	29.0	0.3	1.8	0.1	<1.0	1, 2
625	170	13.0	1.5	6.0×10^{9}	1.06	5.3[illegible]	4.3	17.0	4.8	20.0	2.7	18.0	0.2	1.6	0.1	<1.0	1, 2
670	164	12.0	0.9	5.8×10^{9}	1.17	5.85	2.0	8.6	1.7	9.2	1.2	6.9	0.1	0.4	0.6	<1.0	1, 2

Table C-IX. Shock Layer Attenuation, 40-deg Cone

Time, sec	Altitude, kft	Velocity, kft/sec	f_p, GHz	ν, rad/sec	d(1 ft), in.	d(5 ft), in.	Attenuation, dB: f = 250 MHz, 1 ft	f = 250 MHz, 5 ft	f = 500 MHz, 1 ft	f = 500 MHz, 5 ft	f = 1 GHz, 1 ft	f = 1 GHz, 5 ft	f = 5 GHz, 1 ft	f = 5 GHz, 5 ft	f = 10 GHz, 1 ft	f = 10 GHz, 5 ft	Traject. 1 = Equil. 2 = Trans.
0	300	25.6	2.05	5.2×10^7	0.44	2.20	7.1	27.0	3.3	19.0	1.1	14.0	0.0	0.0	0.0	0.0	1
100	266	25.0	5.80	3.7×10^8	0.44	2.20	26.0	73.0	18.0	97.0	16.0	68.0	2.7	23.0	0.2	0.2	1
150	247	24.0	9.00	9.0×10^8	0.46	2.30	36.0	103.0	35.0	120.0	26.0	104.0	11.0	76.0	2.4	2.6	1
190	236	23.0	10.00	1.3×10^9	0.50	2.51	38.0	115.0	34.0	117.0	30.0	115.0	16.0	99.0	4.3	17.0	1
230	227	22.0	10.00	1.7×10^9	0.52	2.62	37.0	110.0	34.0	114.0	29.0	113.0	14.0	95.0	4.2	16.0	1
275	220	21.0	8.00	1.9×10^9	0.52	2.62	30.0	87.0	26.0	84.0	23.0	90.0	5.7	69.0	1.2	1.6	1
320	214	20.0	6.50	2.1×10^9	0.56	2.82	25.0	78.0	25.0	81.0	21.0	80.0	6.4	49.0	0.2	0.5	1
365	207	19.0	4.50	2.7×10^9	0.61	3.04	18.0	52.0	14.0	55.0	12.0	58.0	2.0	7.2	0.0	0.0	1
0	300	25.6	2.05	5.2×10^7	0.44	2.20	7.1	27.0	3.3	19.0	1.1	14.0	0.0	0.0	0.0	0.0	2
30	280	25.6	4.05	1.8×10^8	0.44	2.20	17.0	52.0	14.0	45.0	8.2	43.0	0.6	9.4	0.0	0.0	2
60	260	25.6	8.00	5.9×10^8	0.44	2.20	31.0	95.0	28.0	84.0	23.0	92.0	8.2	56.0	2.0	5.9	2
90	240	25.6	14.00	1.4×10^9	0.44	2.20	46.0	154.0	48.0	157.0	44.0	172.0	26.0	125.0	16.0	95.0	2
120	220	25.6	20.50	3.0×10^9	0.44	2.20	45.0	147.0	53.0	171.0	54.0	214.0	43.0	196.0	33.0	174.0	2
150	200	25.6	32.00	7.0×10^9	0.44	2.20	47.0	150.0	61.0	200.0	67.0	270.0	72.0	310.0	60.0	290.0	2
170	200	25.0	30.00	6.4×10^9	0.44	2.20	47.0	150.0	58.0	188.0	67.0	270.0	68.0	290.0	60.0	290.0	2
205	200	24.0	25.00	5.9×10^9	0.46	2.30	43.0	128.0	50.0	174.0	59.0	234.0	55.0	263.0	47.0	234.0	2
240	200	23.0	20.00	5.0×10^9	0.50	2.51	41.0	121.0	43.0	141.0	50.0	195.0	42.0	230.0	33.0	192.0	2
275	200	22.0	16.00	4.8×10^9	0.52	2.62	36.0	117.0	33.0	108.0	38.0	147.0	29.0	169.0	25.0	160.0	2
305	200	21.0	12.00	4.0×10^9	0.52	2.62	30.0	92.0	36.0	121.0	27.0	105.0	22.0	131.0	10.0	76.0	2
340	200	20.0	8.00	3.7×10^9	0.56	2.82	24.0	70.0	23.0	74.0	25.0	89.0	10.0	70.0	2.1	7.9	2
375	200	19.0	5.00	3.1×10^9	0.61	2.82	17.0	48.0	16.0	59.0	15.0	64.0	2.8	17.0	0.1	2.2	2
410	200	18.0	3.00	3.0×10^9	0.63	3.14	12.0	37.0	10.0	34.0	6.4	41.0	0.6	1.6	0.0	0.0	1, 2
450	194	17.0	1.70	3.3×10^9	0.65	3.24	4.4	18.0	4.0	21.6	2.0	17.0	0.1	0.5	0.0	0.0	1, 2
495	188	16.0	1.10	3.3×10^9	0.69	3.45	1.6	9.0	1.7	9.0	0.7	6.6	0.0	0.2	0.0	0.0	1, 2
540	182	15.0	0.90	3.9×10^9	0.75	3.77	2.6	8.6	1.3	8.0	0.6	4.1	0.0	0.2	0.0	0.0	1, 2
585	176	14.0	0.60	3.9×10^9	0.82	4.08	1.3	4.7	0.8	4.5	0.4	1.7	0.0	0.0	0.0	0.0	1, 2
625	170	13.0	0.42	3.9×10^9	0.90	4.50	0.6	3.0	0.4	2.2	0.2	0.8	0.0	0.0	0.0	0.0	1, 2
670	164	12.0	0.25	4.1×10^9	0.94	4.70	0.2	0.8	0.1	0.7	0.0	0.3	0.0	1.0	0.5	0.0	1, 2

Table C-X. Boundary Layer Attenuation, 40-deg Cone

Time, sec	Altitude, kft	Velocity, kft/sec	f_p, GHz	ν, rad/sec	d(1 ft) in.	d(5 ft) in.	Attenuation, dB f = 250 MHz 1 ft	f = 250 MHz 5 ft	f = 500 MHz 1 ft	f = 500 MHz 5 ft	f = 1 GHz 1 ft	f = 1 GHz 5 ft	f = 5 GHz 1 ft	f = 5 GHz 5 ft	f = 10 GHz 1 ft	f = 10 GHz 5 ft	Traject 1 - Equil. 2 Trans.
0	300	25.6	-	-	-	-	-	-	-	-	-	-	-	-	-	-	1
100	266	25.0	-	-	-	-	-	-	-	-	-	-	-	-	-	-	1
150	247	24.0	12.3	9.3×10^8	0.19	0.42	30.0	43.0	26.0	36.0	19.0	33.0	6.8	17.00	2.5	10.0	1
190	236	23.0	11.0	1.65×10^9	0.16	0.35	24.0	34.0	22.0	31.0	14.0	23.0	3.8	12.00	1.5	4.3	1
230	227	22.0	9.4	2.0×10^9	0.13	0.30	18.0	27.0	16.0	23.0	12.0	20.0	2.0	7.50	0.4	1.5	1
275	220	21.0	7.0	2.5×10^9	0.12	0.27	12.0	18.0	11.0	17.0	6.3	13.0	0.7	2.20	0.1	0.3	1
320	214	20.0	5.2	3.0×10^9	0.11	0.25	7.5	12.7	6.0	10.0	3.5	7.0	0.3	0.80	0.0	0.1	1
365	207	19.0	3.7	3.7×10^9	0.10	0.22	3.8	7.0	3.0	6.0	1.5	3.0	0.1	0.25	0.8	0.0	1
0	300	25.6	-	-	-	-	-	-	-	-	-	-	-	-	-	-	2
30	280	25.6	-	-	-	-	-	-	-	-	-	-	-	-	-	-	2
60	260	25.6	-	-	-	-	-	-	-	-	-	-	-	-	-	-	2
90	240	25.6	23.00	1.45×10^9	0.160	0.35	39.0	54.0	36.0	60.0	32.0	52.0	17.0	38.0	18.0	30.0	2
120	220	25.6	34.00	3.1×10^9	0.110	0.24	36.0	47.0	34.0	51.0	33.0	51.0	28.0	48.0	16.0	33.6	2
150	200	25.6	51.00	6.4×10^9	0.073	0.16	33.0	42.0	34.0	46.0	34.0	46.0	26.0	44.0	16.0	37.0	2
170	200	25.0	43.00	6.3×10^9	0.074	0.17	30.0	39.0	31.0	42.0	30.0	40.0	20.0	40.0	16.0	34.0	2
205	200	24.0	32.00	6.0×10^9	0.076	0.17	26.0	34.0	24.0	35.0	25.0	33.0	15.0	29.0	10.0	20.0	2
240	200	23.0	24.00	5.7×10^9	0.078	0.18	22.0	28.0	18.0	30.0	18.0	31.0	7.0	22.0	3.3	16.0	2
275	200	22.0	16.00	5.4×10^9	0.080	0.18	17.0	23.0	13.0	21.0	13.0	20.0	5.0	11.0	1.6	5.9	2
305	200	21.0	10.50	5.2×10^9	0.084	0.19	12.0	18.0	9.0	15.0	9.5	13.0	1.5	4.5	0.2	1.0	2
340	200	20.0	6.70	4.8×10^9	0.086	0.19	7.3	12.0	4.5	9.0	4.5	8.0	0.5	1.5	0.2	0.5	2
375	200	19.0	4.30	4.6×10^9	0.088	0.20	3.7	8.3	3.8	6.5	1.8	4.5	0.0	0.3	0.0	0.1	2
410	200	18.0	2.60	4.3×10^9	0.091	0.20	1.6	3.0	1.3	2.5	0.4	1.3	0.0	0.1	0.0	0.0	1, 2
450	194	17.0	1.80	5.3×10^9	0.082	0.18	0.6	1.3	0.5	1.0	0.3	0.6	0.0	0.0	0.0	0.0	1, 2
495	188	16.0	1.05	5.8×10^9	0.080	0.18	0.2	0.4	0.1	0.3	0.2	0.5	0.0	0.0	0.0	0.0	1, 2
540	182	15.0	0.61	6.7×10^9	0.076	0.17	0.1	0.2	0.0	0.1	0.0	0.0	0.0	0.0	0.0	0.0	1, 2
585	176	14.0	0.33	7.4×10^9	0.072	0.16	0.0	0.0	0.0	0.0	0.0	0.0	0.0	0.0	0.0	0.0	1, 2
625	170	13.0	0.16	8.1×10^9	0.067	0.15	0.0	0.0	0.0	0.0	0.0	0.0	0.0	0.3	0.0	0.0	1, 2
670	164	12.0	-	-	-	-	-	-	-	-	-	-	-	-	-	-	1, 2

Table C-XI. Shock Layer Attenuation, 30-deg Cone

Time, sec	Altitude, kft	Velocity, kft/sec	f_p, GHz	ν, col/sec	d(1 ft), in.	d(5 ft), in.	Attenuation, dB: f = 250 MHz, 1 ft	f = 250 MHz, 5 ft	f = 500 MHz, 1 ft	f = 500 MHz, 5 ft	f = 1 GHz, 1 ft	f = 1 GHz, 5 ft	f = 5 GHz, 1 ft	f = 5 GHz, 5 ft	f = 10 GHz, 1 ft	f = 10 GHz, 5 ft	Traject. 1 = Equil. 2 = Trans.
0	300	25.6	0.50	2.5×10^{7}	0.36	1.84	0.10	1.1	0.0	0.3	0.0	0.1	0.0	0.0	0.0	0.0	1
100	266	25.0	1.10	1.9×10^{8}	0.40	1.99	1.50	11.0	0.5	5.7	0.0	1.8	0.0	0.0	0.0	0.0	1
150	247	24.0	1.20	5.0×10^{8}	0.40	1.99	2.30	13.0	0.9	7.1	0.3	2.8	0.0	0.0	0.0	0.0	1
190	235	23.0	1.00	7.2×10^{8}	0.42	2.10	1.80	9.4	0.6	6.6	0.2	1.8	0.0	0.0	0.0	0.0	1
230	227	22.0	0.65	1.0×10^{9}	0.44	2.20	0.80	4.4	0.3	2.0	0.1	0.5	0.0	0.0	0.0	0.0	1
275	220	21.0	0.55	1.1×10^{9}	0.46	2.30	0.60	3.3	0.3	1.5	0.1	0.4	0.0	0.0	0.0	0.0	1
320	214	20.0	0.50	1.2×10^{9}	0.48	2.40	0.50	2.8	0.3	1.2	0.1	0.3	0.0	0.0	0.0	0.0	1
365	207	19.0	0.45	1.5×10^{9}	0.52	2.62	0.45	2.3	0.2	1.1	0.1	0.3	0.?	0.0	0.0	0.0	1
0	300	25.6	0.50	2.5×10^{7}	0.38	1.88	0.10	1.1	0.0	0.3	0.0	0.1	0.0	0.0	0.0	0.0	2
30	280	25.6	1.10	9.0×10^{7}	0.38	1.88	1.20	10.0	0.3	5.0	0.1	1.6	0.0	0.0	0.0	0.0	2
60	260	25.6	2.00	3.0×10^{8}	0.38	1.88	6.30	23.0	2.7	17.0	6.9	11.0	0.0	0.1	0.0	0.0	2
90	240	25.6	3.20	7.9×10^{8}	0.38	1.88	12.50	34.0	8.0	31.0	3.8	25.0	0.2	0.5	0.0	0.0	2
120	220	25.6	5.00	1.6×10^{9}	0.38	1.88	19.00	47.0	15.0	48.0	10.0	44.0	1.4	10.0	0.2	0.4	2
150	200	25.6	7.50	3.6×10^{9}	0.38	1.88	21.00	49.0	19.0	59.0	17.0	64.0	5.4	41.0	1.0	2.2	2
170	200	25.0	6.30	3.4×10^{9}	0.40	1.99	19.00	46.0	17.0	51.0	14.0	65.0	3.4	30.0	0.5	1.6	2
205	200	24.0	4.00	3.0×10^{9}	0.40	1.99	13.00	31.0	11.0	36.0	7.4	34.0	0.7	2.6	0.1	0.4	2
240	200	23.0	2.50	3.0×10^{9}	0.42	2.10	7.10	20.0	5.6	21.0	3.1	18.0	0.2	0.3	0.0	0.2	2
275	200	22.0	1.50	2.7×10^{9}	0.44	2.20	3.50	12.0	2.6	11.0	1.0	7.4	0.1	0.2	0.0	0.1	2
305	200	21.0	1.00	2.4×10^{9}	0.46	2.30	1.90	6.1	1.1	5.9	0.4	2.9	0.0	0.1	0.0	0.1	2
340	200	20.0	0.70	2.1×10^{9}	0.48	2.40	1.00	4.6	0.5	2.9	0.2	1.1	0.0	0.0	0.0	0.0	2
375	200	19.0	0.50	2.0×10^{9}	0.52	2.62	0.50	2.9	0.2	1.6	0.1	0.5	0.0	0.0	0.0	0.0	2
410	200	18.0	0.35	1.7×10^{9}	0.54	2.72	0.32	1.4	0.1	0.7	0.0	0.2	0.0	0.0	0.0	0.0	1, 2
450	194	17.0	0.30	2.0×10^{9}	0.58	2.92	0.24	1.1	0.1	0.6	0.0	0.2	0.0	0.0	0.0	0.0	1, 2
495	188	16.0	0.18	2.0×10^{9}	0.61	3.03	0.10	0.4	0.0	0.2	0.0	0.1	0.0	0.0	0.0	0.0	1, 2
540	182	15.0	0.13	2.1×10^{9}	0.65	3.25	0.00	0.2	0.0	0.1	0.0	0.0	0.0	0.0	0.0	0.0	1, 2
585	176	14.0	0.08	2.2×10^{9}	0.71	3.55	0.00	0.1	0.0	0.0	0.0	0.0	0.0	0.0	0.0	0.0	1, 2
625	170	13.0	-	-	-	-	-	-	-	-	-	-	-	-	-	-	1, 2
670	164	12.0	-	-	-	-	-	-	-	-	-	-	-	-	-	-	1, 2

Table C-XII. Boundary Layer Attenuation, 30-deg Cone

Time, sec	Altitude, kft	Velocity, kft/sec	f_p, GHz	ν, rad/sec	d(1 ft), in.	d(5 ft), in.	Attenuation, dB										Traject. 1 = Equil. 2 = Trans.
							f = 250 MHz		f = 500 MHz		f = 1 GHz		f = 5 GHz		f = 10 GHz		
							1 ft	5 ft	1 ft	5 ft	1 ft	5 ft	1 ft	5 ft	1 ft	5 ft	
0	300	25.6	-	-	-	-	-	-	-	-	-	-	-	-	-	-	1
100	266	25.0	-	-	-	-	-	-	-	-	-	-	-	-	-	-	
150	247	24.0	3.20	6.4×10^8	0.22	0.50	8.1	15.00	4.7	10.0	1.4	5.0	0.0	0.0	0.0	0.0	1
190	236	23.0	2.70	1.0×10^9	0.18	0.41	6.7	11.00	2.8	5.0	1.2	3.0	0.0	0.0	0.0	0.0	1
230	227	22.0	2.20	1.4×10^9	0.15	0.34	3.1	6.70	1.6	2.6	0.3	1.0	0.0	0.0	0.0	0.0	1
275	220	21.0	1.60	1.8×10^9	0.14	0.34	1.2	3.20	0.7	1.5	0.2	0.8	0.0	0.0	0.3	0.0	1
320	214	20.0	1.15	2.1×10^9	0.13	0.30	0.3	0.95	0.4	0.9	0.1	0.3	0.0	0.0	0.0	0.0	1
365	207	19.0	0.85	2.6×10^9	0.12	0.27	0.2	0.60	0.1	0.2	0.0	0.0	0.0	0.0	0.0	0.0	1
0	300	25.6	-	-	-	-	-	-	-	-	-	-	-	-	-	-	2
30	280	25.6	-	-	-	-	-	-	-	-	-	-	-	-	-	-	2
60	260	25.6	-	-	-	-	-	-	-	-	-	-	-	-	-	-	2
90	240	25.6	7.700	9.3×10^8	0.190	0.42	21.0	29.0	16.0	23.0	9.8	18.0	0.3	1.6	0.6	0.2	2
120	220	25.6	10.000	2.2×10^9	0.130	0.20	19.0	26.0	16.0	22.0	11.0	21.0	2.0	7.9	0.7	2.4	2
150	200	25.6	15.500	4.5×10^9	0.086	0.19	18.0	25.0	16.0	24.0	14.0	21.0	3.9	11.0	1.7	5.4	2
170	200	25.0	12.300	4.4×10^9	0.088	0.20	16.0	21.0	14.0	21.0	12.0	19.0	2.5	8.0	0.9	2.8	2
205	200	24.0	8.700	4.2×10^9	0.090	0.20	11.0	17.0	11.0	17.0	7.1	11.0	1.2	3.5	0.2	0.8	2
240	200	23.0	5.700	4.0×10^9	0.094	0.21	6.7	11.0	5.7	10.0	3.3	6.4	0.3	0.9	0.0	0.4	2
275	200	22.0	3.800	3.8×10^9	0.093	0.21	3.5	6.7	3.0	6.0	1.7	3.0	0.0	0.0	0.0	0.1	2
305	200	21.0	2.400	3.7×10^9	0.100	0.22	1.6	3.3	1.3	3.1	0.6	1.4	0.0	0.0	0.0	0.0	2
340	200	20.0	1.550	3.5×10^9	0.100	0.23	0.7	1.5	0.5	1.2	0.2	0.6	0.0	0.0	0.0	0.0	2
375	200	19.0	0.950	3.3×10^9	0.100	0.24	0.3	0.8	0.2	0.5	0.2	0.2	0.0	0.0	0.0	0.0	2
415	200	18.0	0.560	3.1×10^9	0.110	0.24	0.1	0.2	0.1	0.2	0.0	0.0	0.0	0.0	0.0	0.0	1, 2
450	194	17.0	0.360	3.7×10^9	0.097	0.22	0.0	0.1	0.1	0.2	0.0	0.0	0.0	0.0	0.0	0.0	1, 2
495	188	16.0	0.200	4.0×10^9	0.097	0.22	0.0	0.0	0.0	0.0	0.0	0.0	0.0	0.0	0.0	0.0	1, 2
540	182	15.0	0.115	4.7×10^9	0.090	0.20	0.0	0.0	0.0	0.0	0.0	0.0	0.0	0.0	0.0	0.0	1, 2
585	176	14.0	-	-	-	-	-	-	-	-	-	-	-	-	-	-	1, 2
625	170	13.0	-	-	-	-	-	-	-	-	-	-	-	-	-	-	1, 2
670	164	12.0	-	-	-	-	-	-	-	-	-	-	-	-	-	-	1, 2

Table C-XIII. Boundary Layer Attenuation, 20-deg Cone

Time, sec	Altitude, kft	Velocity, kft/sec	f_p, GHz	ν, rad/sec	d (1 ft), in.	d (5 ft), in.	Attenuation, dB: f = 250 MHz, 1 ft	f = 250 MHz, 5 ft	f = 500 MHz, 1 ft	f = 500 MHz, 5 ft	f = 1 GHz, 1 ft	f = 1 GHz, 5 ft	f = 3 GHz, 1 ft	f = 3 GHz, 5 ft	f = 10 GHz, 1 ft	f = 10 GHz, 5 ft	Traject. 1 = Equil 2 = Trans.
0	300	25.6	-	-	-	-	-	-	-	-	-	-	-	-	-	-	1
100	264	25.0	-	-	-	-	-	-	-	-	-	-	-	-	-	-	1
150	247	24.0	0.89	3.4×10^8	0.30	0.68	0.7	1.8	0.2	0.6	0.0	0.0	0.0	0.0	0.0	6.3	1
190	236	23.0	0.74	5.5×10^8	0.25	0.55	0.5	1.2	0.1	0.4	0.0	0.0	0.0	0.0	0.0	0.0	1
230	227	22.0	0.61	7.7×10^8	0.22	0.48	0.3	0.6	0.1	0.2	0.0	0.0	0.0	0.0	0.0	0.0	1
275	220	21.0	0.44	9.5×10^8	0.20	0.44	0.1	0.4	0.1	0.1	0.0	0.0	0.0	0.0	0.0	0.0	1
320	214	20.0	0.31	1.1×10^9	0.18	0.40	0.1	0.2	0.0	0.1	0.0	0.0	0.0	0.0	0.0	0.0	1
365	207	19.0	0.22	1.6×10^9	0.16	0.36	0.0	0.1	0.0	0.0	0.0	0.0	0.0	0.0	0.0	0.0	1
0	300	25.6	-	-	-	-	-	-	-	-	-	-	-	-	-	-	2
30	280	25.6	-	-	-	-	-	-	-	-	-	-	-	-	-	-	2
60	260	25.6	-	-	-	-	-	-	-	-	-	-	-	-	-	-	2
90	240	25.6	2.00	4.9×10^8	0.26	0.59	4.0	9.4	1.7	5.0	0.5	2.0	-	-	-	-	2
120	220	25.6	2.90	1.1×10^9	0.17	0.39	6.3	10.0	3.0	7.3	1.0	3.2	-	-	-	-	2
150	200	25.6	4.20	2.3×10^9	0.12	0.27	6.9	12.0	4.6	8.9	2.2	4.7	-	-	-	-	2
170	200	25.0	3.40	2.2×10^9	0.12	0.27	5.7	8.4	3.1	6.5	1.5	3.2	-	-	-	-	2
205	200	24.0	2.50	2.2×10^9	0.12	0.27	3.3	5.7	1.7	3.8	0.7	1.5	-	-	-	-	2
240	200	23.0	1.60	2.1×10^9	0.13	0.28	1.4	2.8	0.7	1.7	0.2	0.6	-	-	-	-	2
275	200	22.0	1.10	2.1×10^9	0.13	0.29	0.7	1.4	0.3	0.7	0.1	0.3	-	-	-	-	2
305	200	21.0	0.67	2.0×10^9	0.14	0.30	0.3	0.5	0.1	0.3	0.0	0.1	-	-	-	-	2
340	200	20.0	0.42	1.9×10^9	0.14	0.31	0.2	0.2	0.1	0.1	0.0	0.0	-	-	-	-	2
375	200	19.0	0.26	1.8×10^9	0.14	0.32	0.1	0.1	0.0	0.0	0.0	0.0	-	-	-	-	2
410	200	18.0	0.15	1.7×10^9	0.14	0.32	0.0	0.0	0.0	0.0	0.0	0.0	0.0	0.0	0.0	0.0	1, 2
450	194	17.0	-	-	-	-	-	-	-	-	-	-	-	-	-	-	1, 2
495	188	16.0	-	-	-	-	-	-	-	-	-	-	-	-	-	-	1, 2
540	182	15.0	-	-	-	-	-	-	-	-	-	-	-	-	-	-	1, 2
585	176	14.0	-	-	-	-	-	-	-	-	-	-	-	-	-	-	1, 2
625	170	13.0	-	-	-	-	-	-	-	-	-	-	-	-	-	-	1, 2
670	164	12.0	-	-	-	-	-	-	-	-	-	-	-	-	-	-	1, 2

Table C-XIV. Shock Layer Thickness vs Ionization Distance for Cones and Wedges

Time, sec	Altitude, kft	Velocity, kft/sec	30-deg. cone d(1 ft), in.	30-deg. cone d(5 ft), in.	30-deg. cone d(ioniz), in.	40-deg. cone d(1 ft), in.	40-deg. cone d(5 ft), in.	40-deg. cone d(ioniz), in.	50-deg. cone d(1 ft), in.	50-deg. cone d(5 ft), in.	50-deg. cone d(ioniz), in.	30-deg. wedge d(1 ft), in.	30-deg. wedge d(5 ft), in.	30-deg. wedge d(ioniz), in.	40-deg. wedge d(1 ft), in.	40-deg. wedge d(5 ft), in.	40-deg. wedge d(ioniz), in.	50-deg. wedge d(1 ft), in.	50-deg. wedge d(5 ft), in.	50-deg. wedge d(ioniz), in
0	300	25.6	0.38	1.88	>10.0	0.44	2.20	>10.0	0.52	2.62	>10.00	0.73	3.66	>10.0	0.90	4.50	>10.0	1.04	5.22	>10.0
100	266	25.0	0.40	1.99	>10.0	0.44	2.20	6.0	0.54	2.72	3.00	0.73	3.66	>10.0	0.90	4.50	4.0	1.09	5.44	2.9
150	247	24.0	0.40	1.99	>10.0	0.46	2.30	2.5	0.58	2.92	1.00	0.75	3.77	8.0	0.94	4.71	2.2	1.17	5.85	0.9
190	236	23.0	0.42	2.10	>10.0	0.50	2.51	2.0	0.58	2.92	0.90	0.80	3.98	7.0	0.98	4.92	1.8	1.19	5.95	0.7
230	227	22.0	0.44	2.20	10.0	0.52	2.62	1.8	0.58	2.92	0.80	0.84	4.18	6.0	1.04	5.22	1.3	1.28	6.38	0.5
275	220	21.0	0.46	2.30	-	0.52	2.62	1.8	0.65	3.25	0.70	0.86	4.30	6.0	1.04	5.22	1.3	1.34	6.70	0.5
320	214	20.0	0.48	2.40	-	0.56	2.82	1.8	0.71	3.56	0.70	0.92	4.60	7.0	1.07	5.34	1.3	1.38	6.90	0.5
365	207	19.0	0.52	2.60	-	0.61	3.03	2.0	0.73	3.66	0.75	0.96	4.80	-	1.13	5.65	1.5	1.46	7.31	0.5
0	300	25.6	0.38	1.88	>10.0	0.44	2.20	>10.0	0.52	2.62	>10.00	0.73	3.66	>10.0	0.90	4.50	>10.00	1.04	5.22	>10.00
30	280	25.6	0.38	1.88	>10.0	0.44	2.20	10.0	0.52	2.62	6.00	0.73	3.66	>10.0	0.90	4.50	10.00	1.04	5.22	4.00
60	260	25.6	0.38	1.88	>10.0	0.44	2.20	4.0	0.52	2.62	1.50	0.73	3.66	10.0	0.90	4.50	3.00	1.04	5.22	1.50
90	240	25.6	0.38	1.88	8.0	0.44	2.20	1.3	0.52	2.62	0.60	0.73	3.66	4.0	0.90	4.50	1.10	1.04	5.22	0.50
120	220	25.6	0.38	1.88	3.0	0.44	2.20	0.6	0.52	2.62	0.25	0.73	3.66	1.9	0.90	4.50	0.40	1.04	5.22	0.23
150	200	25.6	0.38	1.88	1.5	0.44	2.20	0.3	0.52	2.62	0.11	0.73	3.66	0.6	0.90	4.50	0.23	1.04	5.22	0.10
170	200	25.0	0.40	1.99	1.8	0.44	2.20	0.3	0.54	2.72	0.15	0.73	3.66	0.9	0.90	4.50	0.25	1.09	5.44	0.11
205	200	24.0	0.40	1.99	2.2	0.46	2.30	0.4	0.58	2.92	0.18	0.75	3.77	1.2	0.94	4.71	0.30	1.17	5.85	0.15
240	200	23.0	0.42	2.10	3.0	0.50	2.51	0.4	0.58	2.92	0.20	0.80	3.98	1.8	0.98	4.92	0.40	1.19	5.95	0.18
275	200	22.0	0.44	2.20	-	0.52	2.62	0.5	0.58	2.92	0.25	0.84	4.18	2.0	1.04	5.22	0.50	1.28	6.38	0.20
305	200	21.0	0.46	2.30	-	0.52	2.62	0.8	0.65	3.25	0.30	0.86	4.30	2.5	1.04	5.22	0.60	1.34	6.70	0.25
340	200	20.0	0.48	2.40	-	0.56	2.82	1.0	0.71	3.56	0.40	0.92	4.60	3.0	1.07	5.34	0.80	1.38	6.90	0.30
375	200	19.0	0.52	2.62	-	0.61	3.04	1.5	0.73	3.66	0.60	0.96	4.80	4.5	1.13	5.65	1.00	1.46	7.31	0.40
410	200	18.0	0.54	2.72	-	0.63	3.16	2.0	0.75	3.76	0.8	0.96	4.80	-	1.17	5.85	1.7	1.46	7.31	0.5
450	194	17.0	0.58	2.92	-	0.65	3.24	2.0	0.84	3.98	0.8	0.98	4.92	-	1.26	6.28	1.8	1.54	7.72	0.6
495	188	16.0	0.61	3.03	-	0.69	3.45	-	0.86	4.29	1.0	1.07	5.34	-	1.36	6.80	2.0	1.65	8.25	0.7
540	182	15.0	0.65	3.25	-	0.75	3.77	-	1.00	5.00	1.3	1.15	5.75	-	1.44	7.20	2.5	1.78	8.88	0.8
585	176	14.0	0.71	3.55	-	0.82	4.08	-	1.08	5.08	1.5	1.21	6.05	-	1.44	7.20	-	1.90	9.50	1.0
625	170	13.0	-	-	-	0.90	4.50	-	1.06	5.32	2.0	1.32	6.58	-	1.54	7.72	-	2.06	10.30	-
670	164	12.0	-	-	-	0.94	4.70	-	1.17	5.85	-	1.44	7.20	-	1.67	8.35	-	2.29	11.45	-

REFERENCE

C-1. S. C. Lin and J. D. Teare, "Rate of Ionization Behind Shock Waves in Air. II. Theoretical Interpretations," Phys. Fluids 6, 355-375 (1963).

APPENDIX D

SYSTEM MARGINS

As discussed in Volume I, Section II-D, the free space system margin, which is defined as the amount of plasma attenuation that the reentry vehicle system can tolerate while it effectively transmits information, is a function of frequency. The calculations which lead to the frequency dependence exhibited in Fig. 23 of Volume I are presented here.

The free space system margin M is given by

$$M = 10 \log_{10} [(S/N)_0/(S/N)_T] \tag{D-1}$$

where $(S/N)_0$ is the signal-to-noise ratio neglecting plasma attenuation and $(S/N)_T$ is the threshold signal-to-noise ratio. If we take the noise figure of the receiver to be unity, the link equation may be written

$$(S/N)_0 = \left(\frac{\lambda_0}{4\pi R}\right)^2 \frac{P_T G_T G_R}{k T_e \Delta f L} \tag{D-2}$$

where λ_0 is the free space wavelength, R is the range, P_T is the transmitter power, G_T is the transmitting antenna gain, G_R is the receiving antenna gain, Δf is the rf bandwidth, L represents miscellaneous losses, k is Boltzmann's constant, and T_e is an effective noise temperature given by

$$T_e = 290°K + T_A \tag{D-3}$$

where T_A is the effective antenna temperature.

As discussed in Volume I, parameters were chosen as follows:

$(S/N)_T = 10$

$R = 100$ mi

$\lambda_0 = 0.03$ to 300 m

$P_T = 1$ W

$G_T = 1$

$f = 300$ kHz

$L = 10$

The receiving antenna gain and effective antenna temperature are dependent on frequency, and this dependence is illustrated in Figs. D-1 and D-2. These graphs are intended to be representative rather than to provide ultimate design criteria. The data points of Fig. D-1 were obtained from manufacturer's catalogues and published characteristics. The data of Fig. D-2 were obtained from Refs. D-1, D-2, and D-3. In the frequency range below 10 MHz the noise is largely atmospheric, whereas in the range between 10 MHz and 500 MHz the noise is largely galactic.

The results of the system margin calculation are given in Fig. D-3. As discussed in Volume I, system margins for other transmitter power levels, receiver bandpasses, antenna gains, and ranges can easily be obtained from Fig. D-3 and Eq. (D-2).

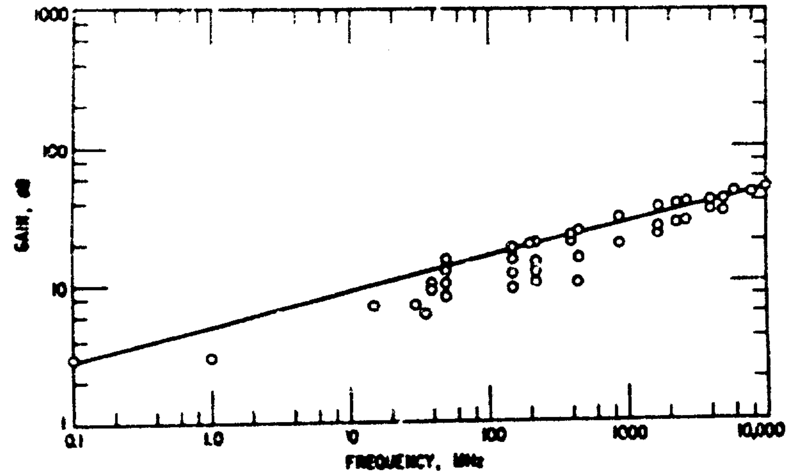

Fig. D-1. Antenna Gain vs Frequency

Fig. D-2. Effective Antenna Temperature

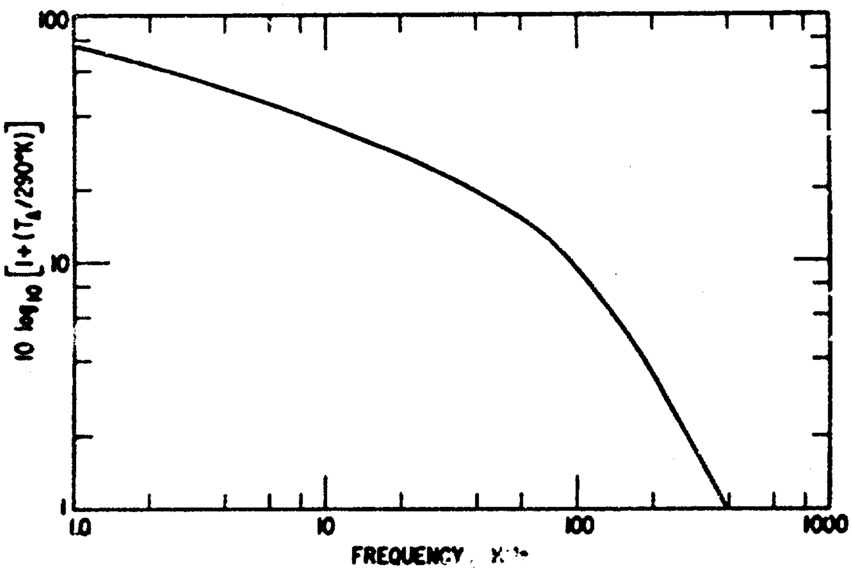

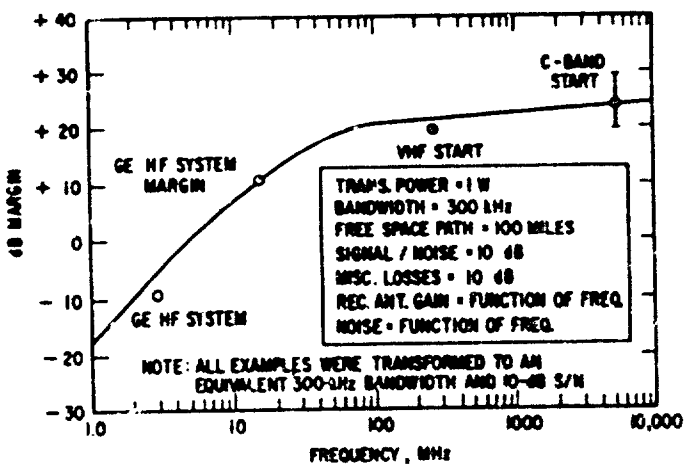

Fig. D-3. Typical Free Space System Margin

REFERENCES

D-1. H. L. Stiltz, Aerospace Telemetry Prentice-Hall, Inc., Englewood Cliffs, N. J., (1961). Chap. 7.

D-2. G. H. Krassner, and J. V. Michaels, Introduction to Space Communication Systems, McGraw-Hill Book Co., Inc., New York (1964). Chap. 4.

D-3. International Telephone and Telegrath Corportation, Reference Data for Radio Engineers, American Book - Stratford Press, New York (1957). Chap. 25.

APPENDIX E

SYSTEM MODIFICATION

Calculations pertinent to the evaluation of the feasibility of increasing the rf power of lifting reentry communications systems are presented in this appendix. The application of the results is presented in Sections III-B, III-D, and III-E of Volume I.

1. POWER AMPLIFIER WEIGHT PENALTY

The weight of a power amplifier over the range of conventional telemetry frequencies may be considered to be directly proportional to both the power output and the operating frequency (Ref. E-1). At 250 MHz, a 6-oz water-cooled tube (EIMAC 4W300B) delivers about 200 W of rf power with an input of about 300 W of dc power. A power supply capable of delivering 300 W for a 10-min period should weigh about 3 lb (this estimate includes batteries and converter). The water required to dissipate 100 W for 10 min is less than 0. 1 lb. Allowing 1 lb for the tube and associated components and 3 lb for the power supply, we estimate the total weight for the 200-W amplifier to be 4 lb. Using this estimate for normalization, we derive the relation

$$W = P_o f(1.25 \times 10^4)^{-1} \text{ lb} \qquad \text{(E-1)}$$

where W is the weight penalty, P_o is the output power in W, and f is the frequency in MHz.

We observe that an EIMAC X-1134 Telemetry Amplifier Package delivers 20 W of CW rf power at 8000 MHz. The package weight is 10 lb, indicating a total weight of 11 lb if we allow 1 lb for a 200-W 28-V source. Our weight-penalty formula gives 13 lb for such a system, and this is taken to indicate that we may use the formula to make sufficiently accurate estimates.

2. BREAKDOWN LIMITATIONS FOR PULSED SOURCES

Radio frequency breakdown limitations for CW sources have been discussed in Volume I, Section II-B-4. Here we determine whether breakdown limitations can be reduced by using a source that is pulsed in such a way that average power remains constant while the duty cycle is reduced.

For pulsed rf energy, breakdown occurs when the ionization rate ν_I multiplied by the pulse-length τ exceeds a certain constant (Ref. E-2). Since the pulse-length is inversely proportional to the peak power, the power is proportional to the square of the electric field E, and the ionization rate is a function of the electric field, we conclude that the condition for avoiding breakdown may be written

$$R = \frac{\nu_I(E)}{E^2} < \text{constant} \qquad \text{(E-2)}$$

Table E-I, which is based on calculations presented in Ref. E-2, indicates that the quantity R defined by Eq. (E-2) is an increasing function of peak power and, therefore, a decreasing function of pulse-length. We conclude that breakdown limitations become more severe for a given pulse of electromagnetic energy as the pulse-length is reduced (see Volume I, Section III-B).

Table E-I. Behavior of Breakdown Parameter R

E (relative)	(E) (relative)	E^2 (relative)	R (relative)
2	1.5	4	0.4
3	15	9	1.7
4	40	16	2.5
5	150	25	6
10	3000	100	30

REFERENCES

E-1. G. E. Mueller, "A Pragmatic Approach to Space Communication," Proc. IRE 48, 557 (1960).

E-2. A. D. MacDonald, "High Frequency Breakdown of Air at High Altitudes," Proc. IRE 47, 436 (1959).

APPENDIX F

COMMUNICATIONS FIN HEAT TRANSFER

In Fig. 25 of Volume I, Section III-C, results of heat transfer calculations are presented to assess the feasibility of the communications fin concept. The relationships used in these calculations are reproduced here. The notation is defined in the referenced literature (Ref. F-1).

1. STAGNATION-LINE HEAT TRANSFER

The heat transfer to the 0.25-in. radius leading edge of the communication fin has been calculated for the entire nonequilibrium trajectory using the following relationship:

$$\dot{q}_{st} = \frac{0.576}{Pr_w^{0.6}}(\rho_e \mu_e)^{0.44}(\rho_w \mu_w)^{0.06}\left(\frac{dU_e}{ds}\right)^{0.5}(h_r - h_w)\left[1 + (Le^{0.52} - 1)\frac{h_D}{h_e}\right] \tag{F-1}$$

This expression is a modification, by Kemp, Rose, and Detra (Ref. F-2), of the original relationship given by Fay and Riddell (Ref. F-3). Conditions at the wall were arbitrarily chosen to correspond to $T_w = 273°K$.

2. FLAT-PLATE HEAT TRANSFER

The heat transfer to the side of the fin and 1 ft from the leading edge has been calculated using the relationship

$$\dot{q} = 1.383\frac{k^*}{x}(Re_x^*)^{1/2}(Pr^*)^{1/3}(h_r - h_w) \tag{F-2}$$

where k^*, Re^*, and Pr^* are evaluated at a temperature T^* given by

$$T^* = \frac{h^*}{c_{p_{ideal}}} = \frac{0.28h_e + 0.5h_w + 0.22h_r}{0.24} \qquad \text{(F-3)}$$

The ideal gas equation of state and the Sutherland viscosity law are assumed. Wall conditions were chosen to correspond to $T_w = 1300°K$. Heat transfer rates calculated were compared with the calculations of Miles and Waldman (Ref. F-4) and were found to be in good agreement.

REFERENCES

F-1. H. H. Koelle, ed., Handbook of Astronautical Engineering, McGraw-Hill Book Co., Inc., New York (1961).

F-2. N. H. Kemp, P. H. Rose, and R. W. Detra, Laminar Heat Transfer around Blunt Bodies in Dissociated Air, AVCO Research Lab. Research Rept. 15. (1958)

F-3. J. A. Fay and F. R. Riddell, "Stagnation Point Heat Transfer in Dissociated Air," AVCO Research Lab. Research Rept. 1 (1957).

F-4 P. Miles and G. Waldman, Laminar Boundary Layer Skin Friction, Heat Transfer and Displacement Thickness Correlations for Sharp Cones, RAD-TM 62-90, Avco Corp., Research and Advanced Development Div., Wilmington, Mass. (November 1962).

APPENDIX G

MAGNETIC WINDOW

Formulas and sample calculations pertinent to magnetic window systems are presented here. The application of these results to the evaluation of magnetic window as a reentry communications system is presented in Volume I, Section III-D.

1. DERIVATION OF FORMULAS

a. COIL GEOMETRY

We envision a coil composed of copper or aluminum wire wrapped around a circular antenna aperture. Figure G-1 is a cross-sectional view of the coil showing the average diameter d, the cross-sectional width a, the aperture diameter b, and the distance to the sheath y.

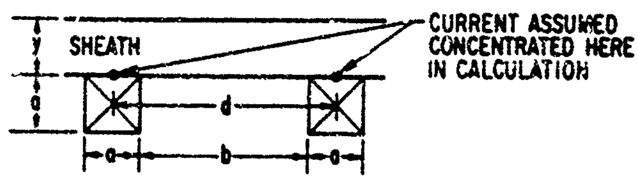

Fig. G-1. Coil Geometry

b. CURRENT REQUIREMENT

The total current I_T in a cross section of the coil is equal to the number of turns in the coil multiplied by the current at the input terminals. The total current requirement is linearly related to the magnetic fie... strength required in the sheath. For our purposes, this relationship is approximated by assuming that the equivalent uniform magnetic field of the coil has the same dependence on the displacement y as the axial field. With this approximation, we obtain

$$\overline{B} \approx \overline{B}_0 \left(1 + \frac{4y^2}{d^2}\right)^{-3/2} \qquad \text{(G-1)}$$

and to complete the specification of the current requirement we estimate

$$\overline{B}_0 \approx \frac{\mu_0 I_T}{d} \qquad \text{(G-2)}$$

In the above expressions, $\overline{B}$ is the average field in the sheath, $\overline{B}_0$ is the average field in the plane of the coil, and μ_0 is the magnetic permeability of free space. (MKS units are used for all quantities except weights, which are given in pounds.)

c. SYSTEM WEIGHT AND APERTURE DIAMETER

The total system consists of the coil, the batteries, and the cooling system. If we assign a weight to the coil-supporting structure equal to 10% of the coil weight, and a weight to the cooling system equal to twice the weight of the water required to dissipate ohmic heat losses, we obtain

$$W = \pi d \left[1.1 \rho A + \frac{I_T^2 rt}{A} \left(\frac{2}{L} + \frac{1}{B} \right) \right] \qquad \text{(G-3)}$$

where

W = system weight, lb

ρ = specific density of conductor, lb/m^3

$A = a^2$ = cross-sectional area of coil, m^2 (see Fig. G-1)

r = resistivity of coil material, ohm-m

t = total time of operation, sec

L = specific heat of vaporization of water, J/lb

B = specific energy capacity of batteries, J/lb

The value of cross-sectional area A is taken as the value that minimizes the system weight. The minimization procedure yields

$$W = 2.2 \times 10^{-2}\, I_T d (r\rho t)^{1/2} \text{ lb}$$

$$A = 3.2 \times 10^{-3}\, I_T (rt/\rho)^{1/2} \text{ m}^2$$

$$b = d - A^{1/2} \text{ m} \qquad \text{(G-4)}$$

We note that system weight is directly proportional to the magnetic field and the square root of the on-time.

The voltage input V_{in} and the current input I_{in} are determined by the number of turns N in the coil; the number of turns is determined by the size of the coil wire. If the cross-sectional area of the wire is σ, we have

$$N = A/\sigma$$

$$V_{in} = N I_T (r\pi d/A)$$

$$I_{in} = I_T/N \qquad \text{(G-5)}$$

2. SAMPLE CALCULATIONS

Representative requirements for a magnetic window system capable of limiting signal attenuation to 40 dB at a station 1 ft from the apex of a wedge with a 50-deg angle of attack have been presented in Volume I, Section III-C-3-b. The estimated parameters of this system were

$d = 4$ in.

$y = 1$ in.

$\overline{B} = 0.16\ \mathrm{Wb/m^2}$ (1600 G)

$t = 500$ sec

We took the following parameters as representative:

$L = 10^6$ J/lb

$B = 1.1 \times 10^5$ J/lb (30 W-h/lb)

$r = 2.2 \times 10^{-8}$ ohm-m (copper)

$r = 3.9 \times 10^{-8}$ ohm-m (aluminum)

$\rho = 2 \times 10^4\ \mathrm{lb/m^3}$ (copper)

$\rho = 6 \times 10^3\ \mathrm{lb/m^3}$ (aluminum)

$\mu_0 = 4\pi \times 10^{-7}$ H/m

Using these values in Eq. (G-4), we find that for a copper coil the system weight is about 17 lb, and the aperture diameter is about 2.5 in. For an aluminum coil, the system weight is about 12.5 lb, and the aperture diameter is about 1.5 in.

As indicated in Volume I, Section IV-B, the evaluation of the magnetic field approximations and aperture effects is designated as a task for a future research effort.

APPENDIX H

COOLANT INJECTION

The various calculations pertinent to the evaluation of coolant injection as an alleviation technique as described in Volume I, Section III-E, are collected here.

1. PROPERTIES OF COOLANTS

Figure H-1 is adapted from Ref. H-1. The data in the figure are discussed in the argument for the selection of water as an injectant in Volume I, Section III-E-1.

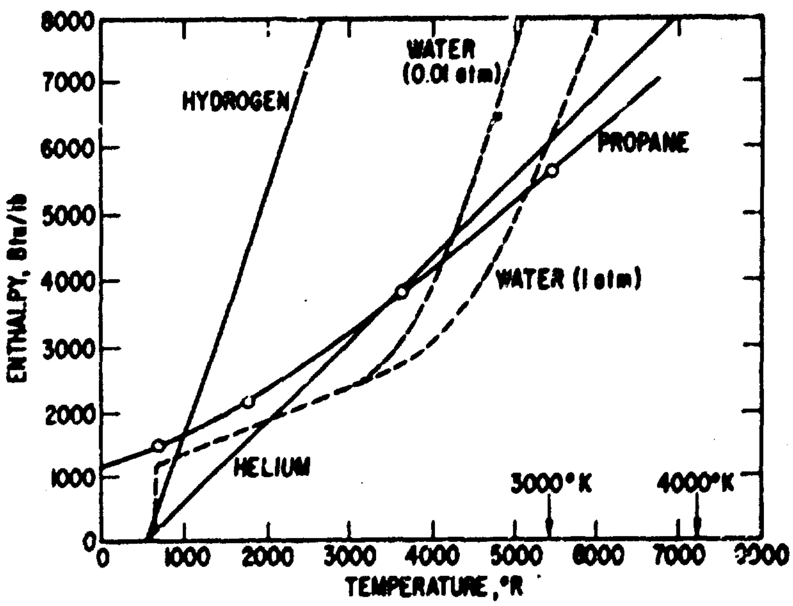

Fig. H-1. Cooling Effectiveness as a Function of Temperature for Various Coolants

2. QUASI ONE-DIMENSIONAL CONSTANT-PRESSURE MIXING PROCESS

As pointed out in Volume I, Section III-E-2-b, we use a technique identical to that of Ref. H-1.

Consider injection into a streamtube as indicated in Fig. H-2.

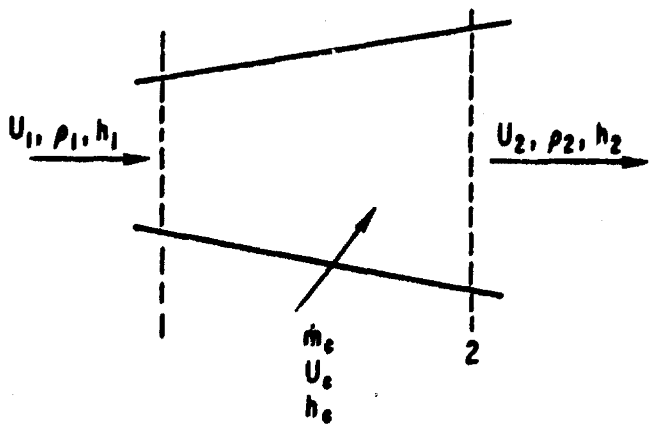

Fig. H-2. Quasi One-Dimensional Mixing Process

The properties are assumed uniform across the cross sections of the streamtube at Stations 1 and 2. The conservation equations are (we assume $U_c \approx 0$)

$$\rho_1 U_1^2 A_1 = \rho_2 U_2^2 A_2 \tag{H-1}$$

$$\rho_1 U_1 A_1 + \dot{m}_c = \rho_2 U_2 A_2 \tag{H-2}$$

$$\rho_1 U_1 A_1 \left[h_1 + \frac{1}{2}\left(U_1^2\right)\right] + \dot{m}_c h_c = \rho_2 U_2 A_2 \left[h_2 + \frac{1}{2}\left(U_2^2\right)\right] \tag{H-3}$$

where ρ is the density; U is the velocity, h is the enthalpy, $\dot{m}_c$ is the injection rate, and A is the cross-sectional area. We now specifically define

$$C = \frac{\rho_{c_2}}{\rho_2} = \text{mass fraction of coolant at Station 2}$$

ρ_{c_2} = density of coolant at Station 2

ρ_{a_2} = density of air at Station 2

$$C_Q = \frac{\dot{m}_c}{\rho_1 A_1 U_1} = \text{mass ratio of injectant to incoming flow}$$

Noting that $C = C_Q/(1 + C_Q)$, we obtain

$$h_2 = [1/(1 + C_Q)] \; [h_1 + C\,(U_1^2/2) + C_Q h_c \qquad \text{(H-4)}$$

Thus, for a given state at Station 1 and an injection ratio C_Q, we may calculate the enthalpy at Station 2, and the pertinent properties of the mixture may be deduced. The electron density is obtained from data for equilibrium air as a function of the temperature and the air density. The collision frequency is obtained (approximately) from the data for equilibrium air (Appendix B, Fig. B-4), where it is assumed that the electron-neutral cross section for helium is seven times greater than that of air on a unit mass basis. Hence, the ordinate in Fig. B-4 is interpreted as $\nu(\rho_o/\rho_{eff})$, where

$$\frac{\rho_{eff}}{\rho_o} = \frac{\rho_{a_2}}{\rho_o} + 7\left(\frac{\rho_{c_2}}{\rho_o}\right) = \frac{1 + 6C}{1 - C} \qquad \text{(H-5)}$$

and the parameter ρ/ρ_o is interpreted as ρ_{a_2}/ρ_o. This is an adequate approximation at the low electron densities of interest, since electron-ion interactions do not contribute significantly to the total electron collision frequency.

The calculation of system weight requirements is described in Volume I, Section III-E-2.

3. ELECTRONEGATIVES AS CATALYSTS

The relaxation time of air in the presence of an electronegative gas is given by $(\sigma_A c_e n_E)^{-1}$, where σ_A is the attachment cross section, c_e is the mean thermal speed of the electrons, and n_E is the number density of the electronegative particles. For SF_6, σ_A is of the order of $10^{-16} cm^2$ (see Appendix I). For a typical reentry case (say, a local velocity about 15 kft/sec and a local pressure of about 0.01 atm) the equilibration time should be about 50 μsec. To obtain a relaxation time of 5 μsec n_E should be about 10^{14}/cc. Since SF_6 is about ten times heavier than water, the water weight is about equal to the weight of air, and the air density is about 10^{17}/cc, we conclude that the injected mixture should contain about a 1% by weight concentration of SF_6 (see Volume I, Section III-F-2-b).

4. ESTIMATE OF DROPLET SIZE

The following empirical expressions for droplet sizes in breakup of liquid jets in air streams are taken from Ref. H-2:

$$\bar{D}/D_o = 3.9(We/Re)^{0.25} \tag{H-6}$$

$$D_{max}/D_o = 22.3(We/Re)^{0.29} \tag{H-7}$$

where

$\bar{D}$ = volume average droplet diameter

D_{max} = maximum droplet diameter

D_o = orifice diameter

$We = \sigma / D_o \rho_s V_s^2$

$Re = D_o V_s / \nu$

σ = surface tension of liquid

ρ_s = air-stream density

V_s = air stream velocity

ν = liquid kinematic velocity

For water

σ = 65 dyn/cm

$\nu = 4.7 \times 10^{-3}$ g/sec-cm (at 60°C)

For

D_o = 0.01 in.

$V_s = 4.5 \times 10^5$ cm/sec

$\rho_s = 1.29 \times 10^{-5}$ g/cc

we obtain

$\bar{D} = 4.45\ \mu$

$D_{max} = 10.8\ \mu$

As discussed in Volume I, Section III-E-2-b, we conclude that a reasonable estimate for the droplet size in the air stream is from 5 to 10μ.

5. EVAPORATION OF WATER DROPLETS

a. Free Molecular Flow

For a droplet of water in air

$$qd^2 = -\frac{1}{6}\rho L \frac{d}{dt}(d^3) \qquad \text{(H-8)}$$

where q is the energy flux, d is the diameter of the droplet, ρ is the specific density of water, and L is the energy per unit mass required for evaporation of water. We readily obtain

$$t_e = \frac{2d_0 L\rho}{q}(1 - f^{1/3}) \qquad \text{(H-9)}$$

where t_e is the evaporation time, d_0 is the initial drop diameter, and f is the ratio of the unevaporated water weight to the initial water weight. The energy flux q is given by

$$q = \sum_i n_i c_i E_i \tag{H-10}$$

and

$$E_i = 2kT + \frac{1}{2}\phi_i \tag{H-11}$$

where the summation is over species, n_i is the particle number density, c_i is the thermal velocity, E_i is the energy per particle, and ϕ_i is the energy obtained from recombination processes. Taking 5.1 eV as the recombination energy for oxygen, 9.8 eV as the recombination energy for nitrogen, and the concentrations listed in Table H-I, we obtain the results listed in Table H-II.

Table H-I. Species Concentration in Air

T, °K	$[N_2]$	[N]	[O]
5950	0.34	0.37	0.28
4000	0.65	-	0.35

Table H-II. Evaporation Times, Free Molecular Flow

Evaporation, %	t_e, µsec	
	5950°K rate	4000°K rate
70	0.062	0.27
80	0.078	0.34
90	0.100	0.44
100	0.190	0.55

b. Continuum Flow

For the continuum case, the energy flux is given by (see Ref. H-3 and references cited therein)

$$q = \frac{N_{Nu} k_f (h_m - h_w)}{d C_{p,w}} \tag{H-12}$$

where

$$N_{Nu} = \frac{2C_{p,m} L}{C_{\hat{p},\hat{v},\hat{f}}(h_m - h_w)} \ln \left(1 + \frac{C_{p,v,f}}{C_{p,m}} \frac{h_m - h_w}{L}\right) \tag{H-13}$$

and

N_{Nu} = Nusselt number

k_f = thermal conductivity of air at $T_f = \frac{1}{2}(T_{drop} + T_{mixture})$

h_m = enthalpy of mixture

h_w = enthalpy of water

$C_{p,m}$ = frozen specific heat of mixture

$C_{p,v,f}$ = specific heat of vapor at T_f

Assuming

$C_{p,m} \approx C_{p,v,f}$

$L \approx 1000$ Btu/lb

$h_m - h_w \approx 5600$ Btu/lb

$k_f \approx 2.2 \times 10^{-5}$ Btu/(ft)(sec)°K

$C_{p,w} \approx 0.24$ Btu/lb

$\rho \approx 62.4$ lb/ft^3

we readily obtain

$$t_e = 4.9 \times 10^{-5}(1 - f^{2/3}) \qquad \text{(H-14)}$$

This approximate formula leads to times t_e of 0.032, 0.038, and 0.049 msec for 80, 90, and 100% evaporation. The application of these results and the results in Appendix H-5-a are discussed in Volume I, Section III-E-2-b.

6. DROPLET DYNAMICS

The equation of motion of a droplet parallel to the air stream is taken as

$$-m \frac{d}{dt} (U_{air} - U_{drop}) = \frac{1}{2} C_D \rho_{air} \frac{\pi d^2}{4} (U_{air} - U_{drop})^2 \qquad \text{(H-15)}$$

where the notation is standard. If the water jet is perpendicular to the flow, x is the distance along a streamline, y is the distance perpendicular to the streamline, and U_i is the initial velocity of the droplets, then

$$\frac{dx}{dt} = U_{air} \left(1 - \frac{1}{1 + \frac{3}{4} C_D \frac{\rho_{air}}{\rho_{drop}} \frac{U_{air}}{d} t} \right) \qquad \text{(H-16)}$$

$$\frac{dy}{dt} = U_i \qquad \text{(H-17)}$$

For U_{air} = 15 kft/sec, $C_D = 2$, $\rho_{air}/\rho_{drop} = 4 \times 10^{-6}$, $d = 10\mu$, and a lateral velocity of 150 ft/sec, the following results are obtained

t, μsec	x, cm	y, cm
20	0.55	0.1
100	9.7	0.5
200	31.2	1.0

These values are the basis for the conclusion that the lateral spreading of the injectant is not severe (Volume I, Section III-E-2-b).

REFERENCES

H-1. R. H. Adams and J. J. Rossi, Research of Aerodynamic Methods of Producing Antenna Windows in a Plasma Sheath, Sci. Rept. No. 1, Mithras Inc. (October 1964).

H-2. R. D. Ingebo and H. H. Foster, Drop-Size Distribution for Cross-current Breakup of Liquid Jets in Air Streams, TN 4087, NACA (October 1957).

H-3. I. E. Beckwith and J. K. Huffman, Injection and Distribution of Liquids in the Flow Fields of Blunt Shapes at Hypersonic Speeds, TM X-989, NASA (August 1964).

APPENDIX I

ELECTROPHILIC SEEDING

Communication difficulties created by the plasmas that surround spacecraft during atmospheric reentry have stimulated considerable research on the effect of electronegative gas injection on the ionization levels in hot gases. The experiments of Carswell and Cloutier (Ref. I-1) indicate that concentrations of SF_6 on the order of the initial electron concentration are very effective in quenching argon plasmas produced by an rf discharge. Conversely, the experiments of Fuhs (Ref. I-2) and Hoffman and Westbrook (Ref. I-3) indicate that SF_6 is much less effective in argon arc jets and seeded nitrogen-oxygen flame plasmas. Theoretical results in this area have been either specialized (Refs. I-2 and I-4) or inconclusive (Ref. I-3). It will be shown here that equilibrium ionization levels of high-temperature air are not significantly affected by the presence of electronegative species but that nonequilibrium levels can be rapidly driven to equilibrium levels by the electron-attachment and charge-transfer mechanism. These conclusions are consistent with the experimental observations, and they provide the basis for evaluating the usefulness of these mechanisms in Sections III-E, III-F, and III-G of Volume I.

1. EQUILIBRIUM

The equilibrium concentrations of the various species in seeded air for a given temperature and pressure are obtained by simultaneously solving the chemical equilibrium equations associated with the pertinent reactions and the appropriate conservation equations. At the temperatures and pressures of interest, the dominant species in air are N_2, N, O_2, O, NO, NO^+, and e^-. If X represents the electronegative component, the mixture will also contain X, X^-, and whatever compounds can be formed by X with N and O. The equilibrium electron density will be a function of temperature, pressure, and initial seed-gas concentration. The exact solution of this problem requires detailed knowledge of chemistry and use of an electronic computer; the problem is considerably simplified, however, if only the reduction in electron density as a function of seed-gas concentration is required. If the optimistic assumption is made that the electronegative species interact only with electrons, and the reasonable assumption is made that the variations in the concentrations of N and O due to the injection of the electronegative gas are negligible, we obtain

$$\frac{n_e[NO^+]}{[N][O]} = K_I$$

$$\frac{n_e(N_E - N_E^-)}{N_E^-} = K_A$$

$$K_I = \frac{\left(n_e^0\right)^2}{[N][O]} \tag{I-1}$$

$$K_A = \left(\frac{2\pi m_e kT}{h^2}\right)^{3/2} \exp(-E_A/kT)$$

$$n_e + N_E^- = [NO^+]$$

where n_e^0 is the initial electron concentration, n_e is the equilibrium electron concentration, N_E is the initial electronegative species concentration, N_E^- is the equilibrium negative ion concentration, K_I is the chemical equilibrium constant for the ionization reaction, K_A is the chemical equilibrium constant for the electron attachment reaction, E_A is the electron affinity of the electronegative species, and the other symbols are standard. These equations lead to

$$\left(\frac{n_e}{n_e^0}\right)^2 = \frac{n_e + K_A}{N_E + n_e + K_A} \gtrsim \frac{K_A}{N_E + K_A} \tag{I-2}$$

This expression differs from the analogous equation of Ref. I-3 because here account has been taken of Le Chatelier's principle — as the electronegative component removes electrons, the reaction $N + O \rightarrow NO^+ + e^-$ will produce more electrons. Known electron affinities do not exceed 4 V, therefore the limit of the attachment mechanism effectiveness can easily be calculated. Such calculations for 10% concentrations of 4-V electronegative species in air have been performed for temperatures and pressures characteristic of the reentry environment, and the results are presented in Fig. I-1. The curve labelled $\rho/\rho_0 = 10^{-2}$ compares favorably with exact calculations (Ref. I-4) for 5% concentrations of F_2, thus indicating the validity of the assumptions described. The electronegative concentrations required for a reentry system were calculated from Eqs. (I-1) and (I-2), and the results are presented in Volume I, Section III-F-2.

2. NONEQUILIBRIUM

When the electron density is higher than the equilibrium level, the approach to equilibrium in the presence of an electronegative component is given by

$$\frac{dn_e}{dt} = -\alpha_R n_e^2 - \alpha_A N_E n_e \qquad \text{(I-3)}$$

where α_R is the electron-ion recombination rate constant, and α_A is the electron attachment rate constant. As pointed out by Carswell and Cloutier, we may assume that the rate at which the electronegative component transfers electrons to positive ions is much faster than the attachment rate, thus N_E may be regarded as a constant. If we make the transformation $t \rightarrow \alpha_R n_e^0 \tau$ so that, in the absence of the electronegative component, the electron density decays to one-half its initial value when $\tau = 1$, we obtain the solutions given in Fig. I-2, where the seeding parameter r represents the ratio $\alpha_A N_E / \alpha_R n_e^0$. The experimental curves presented by Carswell and Cloutier are in agreement with the theoretical curves for a seeded argon plasma when the reasonable

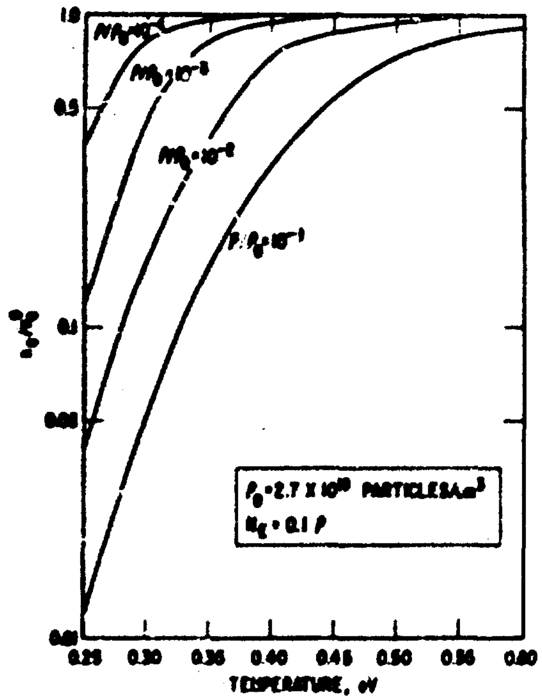

Fig. I-1. Reduction of Equilibrium Electron Concentrations in Seeded Air

Fig. I-2. Reduction of Non-equilibrium Electron Concentrations in Seeded Ionized Gases

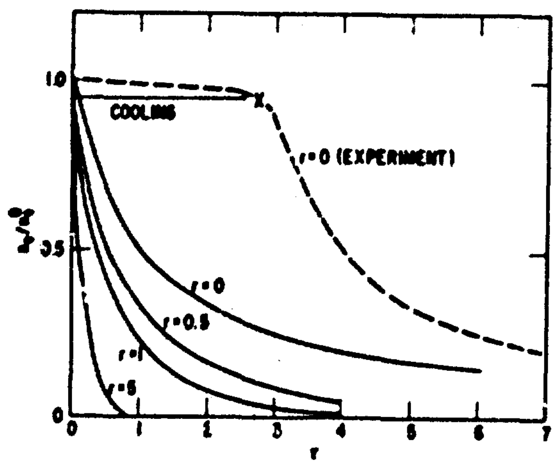

assignments α_R, $\alpha_A \sim 10^{-9}$ are made (Refs. I-5 and 6). (The value for α_A is based on an electron attachment cross section of $10^{-16} cm^2$.) The dashed line in the figure represents the measured curve for the unseeded plasma — the discrepancy is probably due to the fact that the electrons must be cooled before they can recombine with positive ions (the reported initial temperature was 7×10^4 °K).

It may be concluded from these considerations that electrophilic seeding is not effective in reducing equilibrium electron density levels in nonexpanding flows but that it can be effective in catalyzing the electron-ion recombination process in expanding flows or in flows which have been cooled by injection of foreign material. The specific application of these conclusions to the reentry communications problem have been discussed in Volume I, Section III-E, III-F, and III-G.

REFERENCES

I-1. A. I. Carswell and G. G. Cloutier, "Supersonic Plasma Streams Seeded with Electronegative Gases," Phys. Fluids 7, 602 (1964).

I-2. A. E. Fuhs, Thermal Ionization and Electronegative Species, TDR-165(3153)TN-2, Aerospace Corp. (September 1962).

I-3 J. Hoffman and E. A. Westbrook, "Flame Plasma Seeded with Sulfur Hexafluoride," Phys. Fluids 8, 1410 (1965).

I-4. A. R. Hochstim, "Electron Concentration in Closed Form For High Temperature Air and Air Additives," Planetary and Space Sciences 6, 79 (1961).

I-5. I. S. Buchel 'nikova, "Cross Sections for the Capture of Slow Electrons by O_2 and H_2O Molecules and Molecules of Halogen Compounds," JETP (USSR) 35, 783 (1959).

I-6. L. B. Loeb, "The Recombination of Ions," Handbuch der Physik, Band XXI, Springer-Verlay, Berlin (1956).

APPENDIX J

QUASI-OPTICAL AND OPTICAL SYSTEMS

The power requirements for the systems described in Volume I, Section III-I are derived here.

1. MILLIMETER SYSTEM

The power P_R required at the input of a state-of-the-art 95-GHz receiver is given by

$$P_R = (S/N)(NF)kT\Delta f \qquad (J-1)$$

where

$S/N = 10$ (signal-to-noise power ratio)

$NF = 40$ (receiver noise figure)

$kT = 4 \times 10^{-21}$ W/Hz (noise power per cycle)

$\Delta f = 300$ kHz (receiver bandpass)

We readily obtain $P_R = 4.8 \times 10^{-13}$W. The required output power P_T for an omnidirectional system is given by

$$P_T = 4\pi \, (R^2/A_R) \, P_R \qquad (J-2)$$

where R is the range, and A_R is the effective area of the receiver antenna. For a range of 100 miles and an area of 200 ft^2 we obtain $P_T = 9$ mW. Allowing for miscellaneous losses of 10 dB; we estimate a requirement of 90 mW for an omnidirectional clear-weather system. This estimate is discussed in Volume I, Section III-1-1.

2. INJECTION LASER SYSTEM

The signal-to-noise ratio at the output of a photomultiplier is given by

$$S/N = \frac{I_S^2}{2e\Delta f(\bar{I}_S + \bar{I}_B + \bar{I}_D)} \qquad \text{(J-3)}$$

where I_S is the current due to the signal, I_B is the current due to the background radiation, and I_D is the dark current of the tube. In this case, the dark current is negligible, and the required received power is given by

$$P_R = (h\nu/q)(S/N)\Delta f\{1 + [1 + (2qP_B/h\nu\Delta f)(S/N)^{-1}]^{1/2}\} \qquad \text{(J-4)}$$

where P_B represents the background radiation power, $h\nu$ is the photon energy, q is the quantum efficiency of the photomultiplier, and Δf is the bandpass of the video system.

The noise power is given by

$$P_B = I_D\Omega_R A_R B + I_V (A_V/R^2) A_R B \qquad \text{(J-5)}$$

where

I_D = spectral density of daylight noise $\approx 10^{-3}$ W $sr^{-1} m^{-2} \text{Å}^{-1}$

I_V = spectral density of vehicle radiation ≈ 10W $sr^{-1} m^{-2} \text{Å}^{-1}$

A_R = receiving aperture $\approx 1\ m^2$

B = optical filter bandpass ≈ 10Å

Ω_R = receiving field of view $\approx 10^{-6}$sr using the indicated estimates, we obtain

$$P_D \approx 10^{-8} W \text{ (daylight noise)}$$

$$P_V \approx 2 \times 10^{-8} W \text{ (vehicle noise)}$$

$$P_B \approx 3 \times 10^{-8} W$$

Taking $q \approx 3 \times 10^{-3}$, $h\nu = 2.2 \times 10^{-19}$J, and $\Delta f = 10^8$ Hz (corresponding to a pulse length of 10 nsec), we obtain $P_R \approx 3 \times 10^{-8}$W. If atmospheric losses are estimated as 6 dB, a requirement of 50 kW pulses for an omnidirectional transmitting system with a range of 100 miles is indicated. If the transmitted power can be concentrated in a beam with a width of about 10 deg, the peak power requirement is reduced by a factor of about 500, indicating a requirement for 100-W pulses. As discussed in Volume I, Section III-I-2, this estimate is a reasonable requirement for future systems.

UNCLASSIFIED
Security Classification

DOCUMENT CONTROL DATA - R&D

(Security classification of title, body of abstract and indexing annotation must be entered when the overall report is classified)

1. ORIGINATING ACTIVITY (Corporate author) Aerospace Corporation El Segundo, California	2a. REPORT SECURITY CLASSIFICATION Unclassified 2b. GROUP

3. REPORT TITLE
LIFTING REENTRY COMMUNICATIONS: VOLUME II. SYSTEMS CALCULATIONS

4. DESCRIPTIVE NOTES (Type of report and inclusive dates)

5. AUTHOR(S) (Last name, first name, initial)
Dix, Donald M., Golden, Kurt E., Taylor, Edward C., Koplin, Marc A., and Caron, Paul R.

6. REPORT DATE September 1966	7a. TOTAL NO. OF PAGES 73	7b. NO. OF REFS 27

8a. CONTRACT OR GRANT NO. AF 04(695)-669	9a. ORIGINATOR'S REPORT NUMBER(S) TR-669(6220-10)-3, Vol II
b. PROJECT NO.	
c	9b. OTHER REPORT NO(S) (Any other numbers that may be assigned this report)
d	SSD-TR-66-73, Vol II

10. AVAILABILITY/LIMITATION NOTICES
This document is subject to special export controls and each transmittal to foreign governments or foreign nationals may be made only with prior approval of SSD(SSTRT).

11. SUPPLEMENTARY NOTES	12. SPONSORING MILITARY ACTIVITY Space Systems Division Air Force Systems Command Los Angeles, California

13. ABSTRACT

Calculations supporting the lifting reentry communications systems study are described in this volume. The application and interpretation of these calculations is presented in Volume I of this report. These calculations include the study of lifting reentry trajectories, aerodynamic calculations, signal attenuation, system margins, system modifications, communications in heat transfer, magnetic window, coolant injection, electrophilic seeding, and quasi-optical and optical systems.

DD FORM 1473 (FACSIMILE)

UNCLASSIFIED
Security Classification

14. KEY WORDS
Communications Systems Reentry Communications Lifting Reentry Antenna Window Aerodynamics RF Attenuation RF Breakdown Aerodynamic Shaping Fluid Injection Magnetic Window Electrophilic Seeding Millimeter Waves Optical Communications Systems High-Frequency Communications Communications Blackout

Abstract (Continued)